A Study of the Effect of Temperature on Direct Methanol Fuel Cells

A Major Qualifying Project:

Submitted to the faculty of
Chemical Engineering Department
Worcester Polytechnic Institute
in partial fulfillment of the requirements for the
Degree of Bachelor of Science

By

_____
Philip Cox

_____
Margaret Fulton

_____
Christopher LaBarre

April 28th, 2011

Approved by:

_____
Prof. Ravindra Datta, Advisor

Table of Contents

Table of Figures

Abstract

Direct Methanol Fuel Cells (DMFC) typically operate using Nafion-based Membrane Electrode Assemblies (MEAs) up to 100°C. Above this temperature, Nafion begins to degrade, hindering performance. Because temperature improves fuel cell performance PBI-based MEAs were investigated for an intermediate range temperature DMFCs. Nafion MEA performance curves confirmed the relationship between temperature and performance. However, polarization plots for PBI MEAs could not be generated. Despite this, PBI exhibited a sustained current density of 900 mA/cm^2 at 0.10 V using hydrogen.

Chapter 1: Introduction

Fuel cell technology was first used commercially in the 1960's when the United States space program chose to implement the technology rather than rely on other technologies like nuclear power, much more dangerous or solar power, which are much more expensive (Fuel Cell & Hydrogen Energy Association). However, fuel cell technology has been in existence for much longer. In 1839, Sir William Grove built the first fuel cell and titled it a "gas battery" (FCTec Home Page). With numerous improvements over the past 170 years, fuel cells have the potential to be one of the most efficient and environmentally friendly power generation devices (Cheddie et al., 2006).

Today, there are many types of fuel cells, including: Phosphoric Acid fuel cell (PAFC), Proton Exchange Membrane fuel cell (PEM), High Temperature Proton Exchange Membrane fuel cell (HT-PEM), Molten Carbonate fuel cell (MCFC), Solid Oxide fuel cell (SOFC), Alkaline fuel cell (AFC), Direct Methanol fuel cell (DMFC), Regenerative fuel cell, Zinc Air fuel cell (ZAFC), Protonic Ceramic fuel cell (PCFC), and Microbial fuel cell (MFC) (FC2K, 2000). For the purposes of this paper, the focus will mainly be on Direct Methanol Fuel Cell (DMFC) technology.

Fuel cell technology currently has various applications in industry. For example, DMFCs can be found in portable electronics, such as cellphones and laptops (Toshiba's methanol fuel cell, 2004). One of the main advantages to having a DMFC run one's cell phone or laptop is that the fuel cell will allow the unit to run for longer than a standard battery (FC2K, 2000). Other types of fuel cells can be found in much larger applications, such as running hospitals, office buildings, or stores. In most applications, especially large scale, hydrogen is the fuel source;

hydrogen fuel cells are very popular for use in cars and buses (Transforming the Energy Network). Fuel cells are an attractive energy source because they produce lesser amounts of greenhouse gases especially when compared to gasoline run vehicles.

Figure 1, below, summarizes six of the main types of fuel cells and gives some idea of the typical operating temperature. Essentially, hydrogen and oxygen are combined in the fuel cell to produce water, small amounts of CO_2 and electricity (Basic Overview, 2008). The fuel source containing hydrogen is fed into the anode side of the fuel cell while oxygen is fed to the cathode side. At this point the gases pass through the gas diffusion layer, which will regulate the flow as well as store electrons. The catalyst, usually composed of platinum, breaks down the hydrogen or methanol into a number of protons and electrons. The protons pass through the electrolyte and the electrons travel to the cathode via an external circuit, which creates an electric current. At the cathode, the protons and electrons react with the oxygen, which creates water. In Figure 1, the third set of reactions down shows the process of a DMFC.

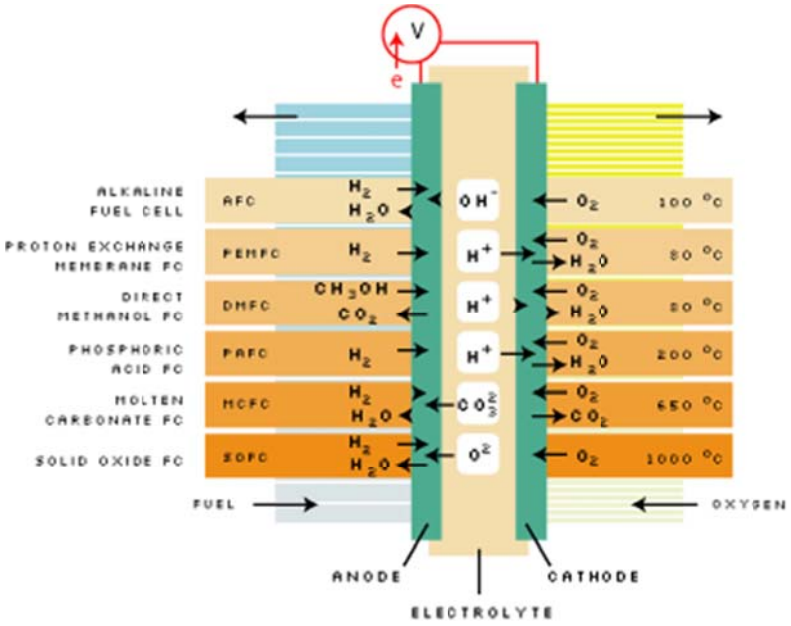

Figure 1: Fuel Cell Model (US Fuel Cell Council)

One of the largest advantages to fuel cell technology is their low emissions. As can be seen in Figure 2, fuel cells significantly less emissions than their competitors. A typical fossil fuel plant produces almost 25 pounds of pollutants per 1000 kWh, whereas the fuel cell will produce much less than 1 pound of pollutant per 1000 kWh (DOE- Fossil Energy: Office of Fossil Energy Home Page, 2010).

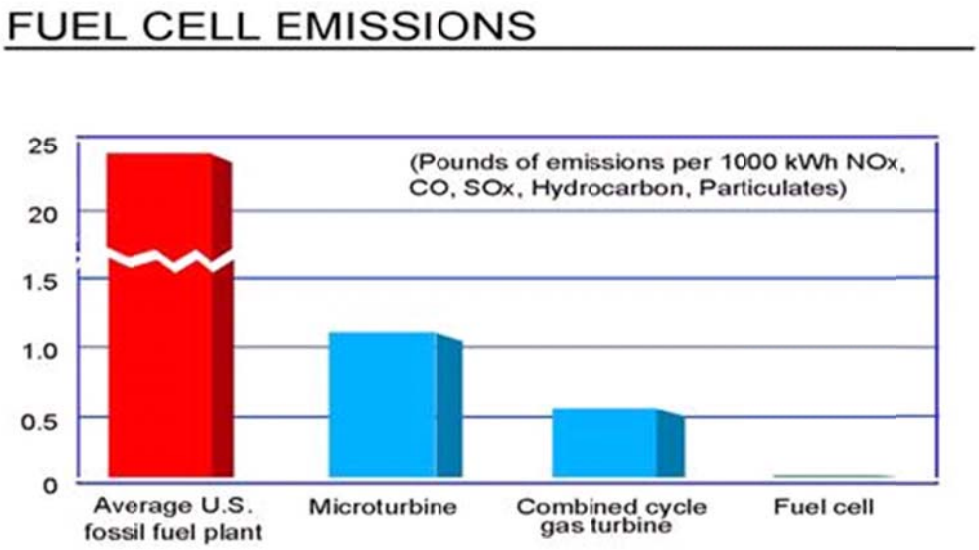

Figure 2: Comparison of Emissions (DOE- Fossil Energy: Office of Fossil Energy Home Page, 2010)

Fuel cells in vehicles that run on hydrogen stored on board the vehicle produce zero pollutants, the only byproduct being water vapor (Fuel Cell & Hydrogen Energy Association). In addition, using fuel cells in trucks to power air conditioners and accessories, emissions could be reduced by up to 45% (FC2K, 2000). If fuel cells were used in Class 8 trucks, 670 million gallons of diesel fuel and 4.64 million tons of CO_2 could be saved per year.

Direct Methanol Fuel Cells

The direct methanol fuel cell (DMFC) uses methanol and O_2 as fuel sources and a polymer electrolyte membrane (PEM) to force an external electrical circuit. A DMFC typically runs at temperatures between 50 to 120°C and has efficiencies of around 40%. (USFCC) This varies from the generic hydrogen PEM fuel cell, which typically runs at 80°C and has an efficiency of 40% to 50%.

Mechanism

DMFC's generate electrical power via an oxidation and reduction reaction, as shown in Figure 3. In the oxidation reaction, methanol is oxidized in the presence of water and a catalyst as shown below. Hydrogen ions are formed at the anode electrode. The reduction reaction at the cathode utilizes supplied oxygen and the protons from the methanol dissociation to form water.

Anode Oxidation	$\mathbf{CH_3OH + H_2O \rightarrow 6\,H^+ + 6e^- + CO_2}$
Cathode Reduction	$\mathbf{\frac{3}{2}O_2 + 6H^+ + 6e^- \rightarrow 3H_2O}$
Overall Reaction	$\mathbf{CH_3OH + \frac{3}{2}O_2 \rightarrow 2H_2O + CO_2}$

Figure 3: Reaction Mechanisms

Diluted liquid methanol flows through a flow chamber to the anode, passes through the anode gas diffusion layer and comes in contact with the platinum/ruthenium catalyst. Unreacted methanol and water exits the anode through a waste stream. Similarly, oxygen or air flows to the cathode gas diffusion layer and then comes in contact with a platinum catalyst.

The bipolar plates, made of graphite, duals as a casing for the fuel cell MEA and are relatively cheap yet durable electrical conductors (Fuel Cell Store, 2011). Graphite contains rows of carbon that share electrons covalently and allows for an electrical current to form when there is a difference in voltage. The voltage can be induced using a load box connected to the bipolar plates through electrodes. The positive electrode is connected to the cathode plate whereas the negative electrode connects to the anode plate. This setup allows for control of the voltage differential across the plates and for measuring the electrical current.

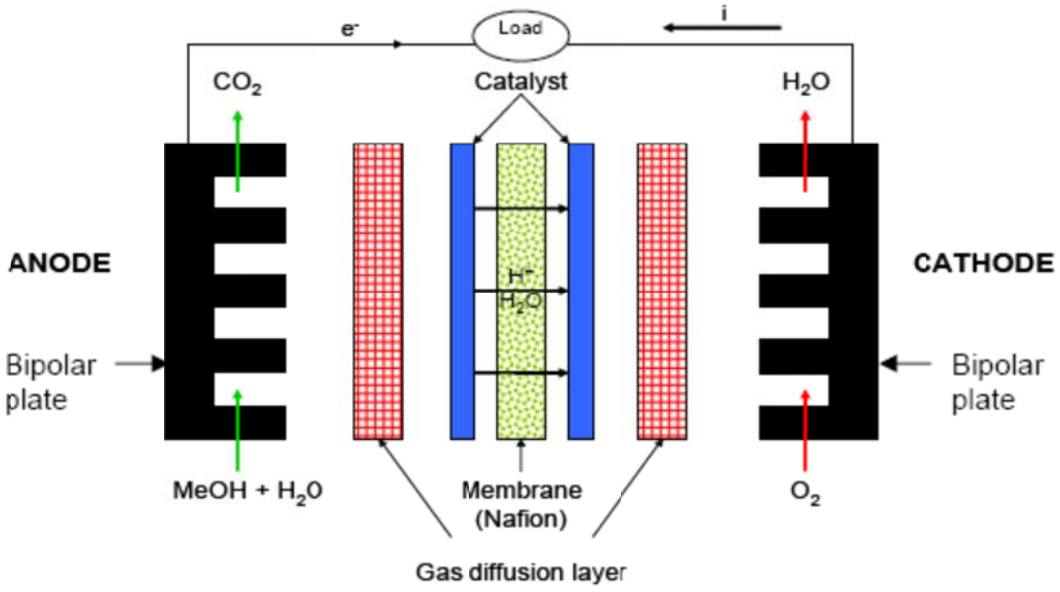

Figure 4: Schematic of DMFC (Hackguard, 2005)

Etched into each bipolar plate is a flow channel, also referred to as a serpentine pattern, which increases methanol contact to the anode electrode.

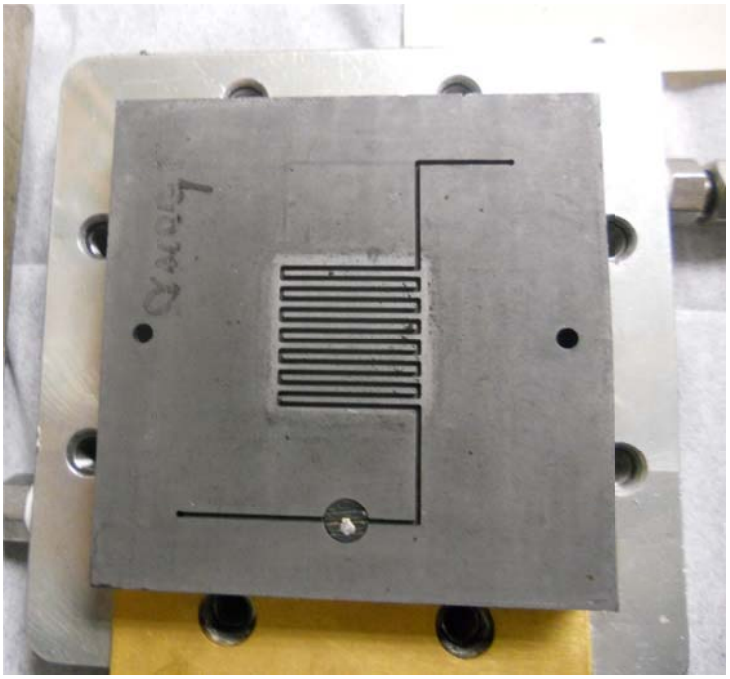

Figure 5: Serpentine pattern on bipolar plate

The gas diffusion layer (GDL) is a porous material that facilitates contact between the methanol-water solution and the catalyst (Han-Kyu Lee, 2003). Carbon cloth is often used as the diffusion layer because the carbon-carbon bonds allow for efficient electron conduction. An ideal GDL allows for uniform permeation across the plane in contact with the catalyst (Hai, 2005). Additionally, the GDL serves to protect the catalyst from cracking by acting as a barrier and dampening heat energy. Catalyst cracking reduces the permeative selectivity of the system and increases the rate of methanol crossover, which will be discussed later.

The catalyst reduces the amount of energy required for each half reaction to occur (Garcia, 2004). Figure 6 helps demonstrate the effect of catalysis on a reaction. At lower energies of activation a higher yield of product can be achieved per unit time.

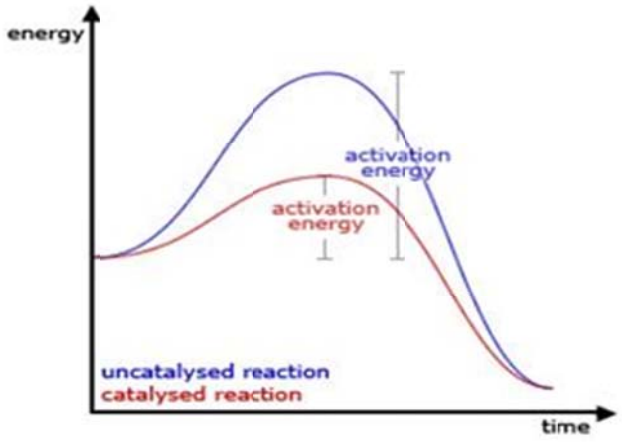

Figure 6: Energy of Activation (Extend 2011)

The Proton Exchange Membrane (PEM) acts as a proton transport medium, carrying protons across the membrane from anode to cathode electrode. The membrane must have sufficient tensile strength to remain structurally intact under pressure and high temperatures. PEM also duals as a barrier between the anode and cathode fuels. However, the PEM does a poor job keeping the fuels separate; Vilekar et al. has shown that hydrogen is able to permeate through the PEM, reducing the Open Circuit Voltage (OCV) from its thermodynamic voltage (1.2V) to about 1.0V (S.A. Vilekar, 2010). The average OCV for DMFCs is even further reduced to ~0.6V due to the inability of PEMs to stop methanol crossover.

PEMs conduct protons and force an electrical current through a loop to the cathode. The polarization curve shown in Figure 7 shows a typical Nafion 117 membrane's performance. Current density is a calculated value corresponding to the current measured from a load box located in series with the loop.

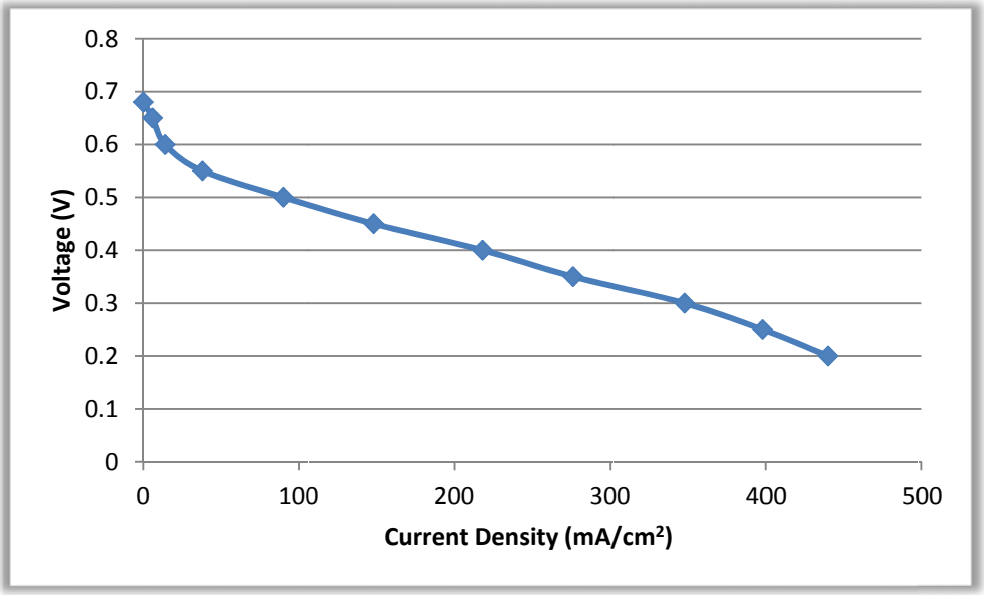

Figure 7: Polarization curve for Nafion 117 Membrane, 3M, 2ml/min, 70°C

Issues

Although DMFCs use a more convenient fuel source then the H_2-O_2 PEMFCs there are several issues that need to be addressed. The overall performance of a DMFC is impaired by methanol crossover, high overpotential and CO poisoning of the anode (Lobato, P., Rodrigo, & Linares, 2009).

Methanol crossover occurs when methanol from the anode side passes through the PEM to the cathode either via diffusion or electro-osmotic drag (Pivovar, 2006). Crossover allows for the

oxidation of methanol to occur at both electrodes reducing fuel efficiency and creating an anode overpotential. Overpotential refers to the difference between the theoretical maximum potential and the actual potential of the bipolar plate.

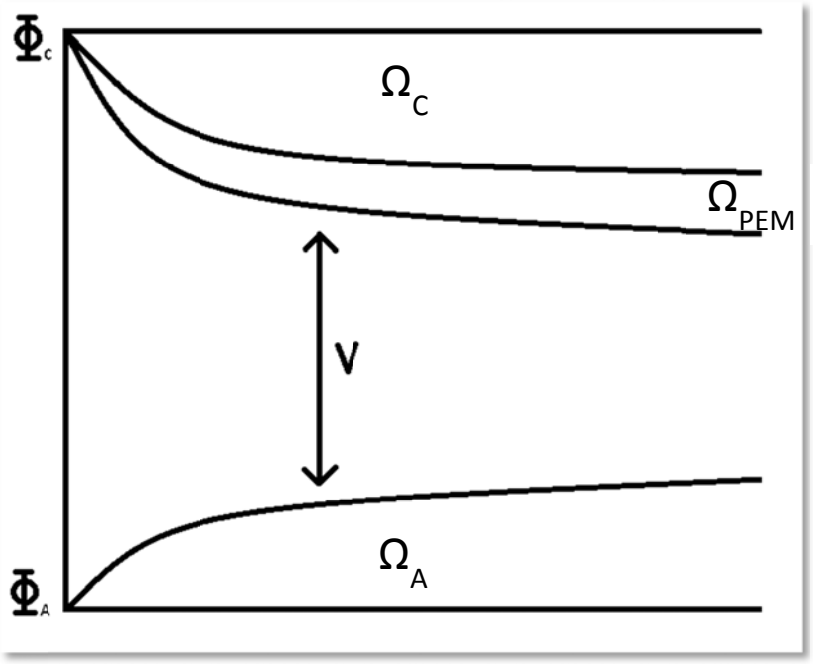

Figure 8: Fuel Cell Overpotential

Both anode and cathode have overpotential. Further contributing to the drop in DMFC performance is ohmic loss; as current density increases, voltage proportionally increases based on the applied resistance and V = IR.

$$J_{MeOH} = -D_{MeOH}\frac{\partial C}{\partial z} \qquad < 1 >$$

Equation < 1 > is methanol flux across the membrane; methanol thermodynamically wants to diffuse along a gradient from higher concentration to lower. This gradient is a natural product of

the PEM acting as a barrier to methanol or hydrogen. Researchers have varied the thickness of the membrane in an effort to reduce dC/dz and have found that thickness will alleviate crossover but at reduced proton conductivity (Jin Hu, 2008).

A DMFC relies on water as a reactant at the anode and is a product of the cathode. Both instances will be referred to under water management, which is another issue affecting DMFC performance. Liquid water readily adheres to pores in the GDL which creates mass transfer limitations for gas flow (Han-Kyu Lee, 2003). Vapor based DMFCs are an attractive option because of the higher kinetics compared to the sluggish kinetics of liquid based.

Chapter 2: Literature Review

Nafion Based MEAs

DMFCs have a variety of parameters which affects its overall performance. The types of parameters include: methanol concentration, the operating temperature of the fuel cell, the flow rate methanol, and membrane thickness. By optimizing these parameters, high DMFC performance can be obtained while keeping methanol crossover, along with the crossover flux, low.

One of the parameters that can be changed to help improve DMFC performance is the concentration of methanol. Jung et al. found that using a higher concentration of methanol improved voltage and power density at higher current densities (Jung et al). As shown in Figure 9, a run at 50^{o}C indicates that 3M methanol performed the best. Additionally, the voltage and power density increased with increasing concentration at high current densities. This happens because there is more methanol to react and thus more power per unit volume to react. However, the OCV was lower as the concentration of the methanol increased because at lower current densities there is less methanol that is needed to react, therefore there is not as much crossover.

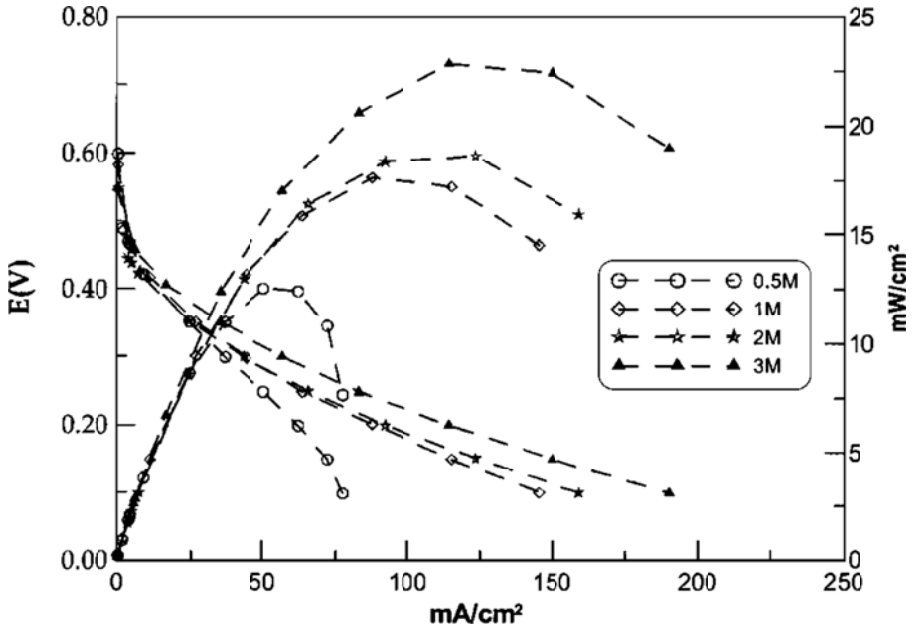

Figure 9: Results of Various Methanol Concentrations at 50^{O}C (Jung et al., 2005)

The authors also obtained a polarization plot at 80^{o}C. According to Figure 10 an increase in temperature shifted the optimal methanol concentration to 1M rather than 3M.

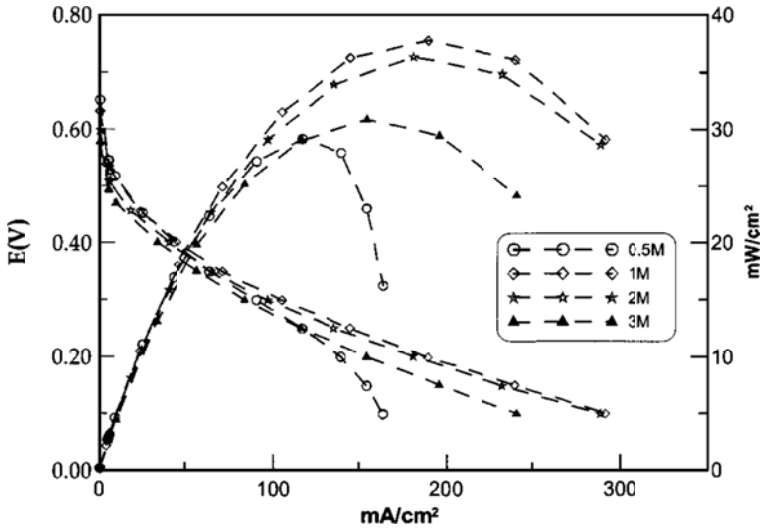

Figure 10: Results of Various Methanol Concentrations at 80^{O}C (Jung et al., 2005)

This implies that methanol crossover is more significant at higher methanol concentrations and higher temperatures. As the operating temperature increases it helps to

increase the reactions of methanol with higher concentrations because the catalyst is more prone to carbon monoxide poisoning. The increase in temperature allows for more protonation in the catalyst which helps to increase performance but at the same time allows a higher chance to have methanol crossover (Jung et al.). Figure 11 shows similar results done by Jung et al. which shows the effects of methanol concentration and operating temperature of a DMFC (Jung et al.). The fuel cell was operated at a temperature of 120^{o}C. Like Figure 10 the highest methanol concentration did not produce the best results; 2.5M performed better than the 4M methanol and 0.5M methanol feeds. This results show that there is a more consistent performance when there is a balance between the methanol concentration and the temperature at which the fuel cell is being operated. Another point to mention is that the OCV decreased with increasing methanol concentrations.

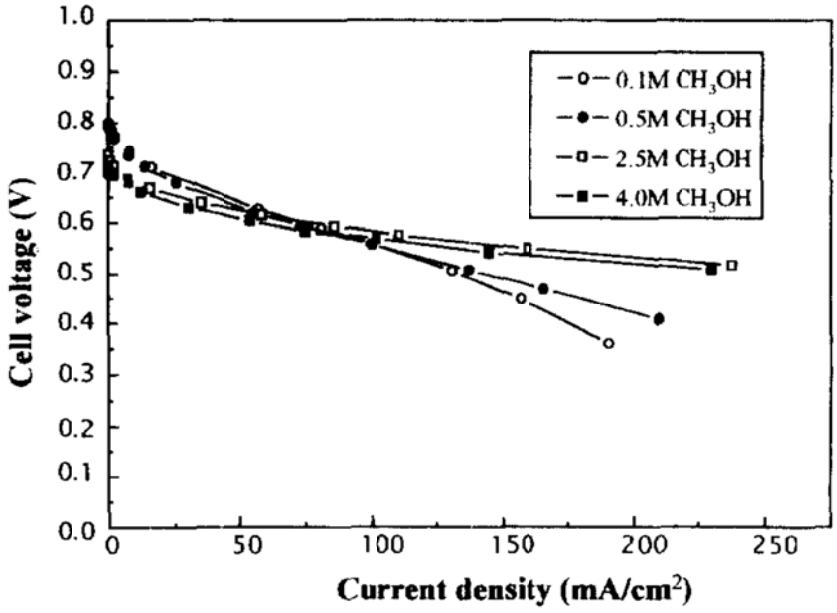

Figure 11: Results of Various Methanol Concentrations at 120^{O}C (Jung et al., 1998)

Temperature strongly influences the performance of the fuel cell. Figure 12 shows the effect of temperature on a DMFC using a Nafion 112 membrane and 1M methanol. The increase in the temperature of the fuel cell showed an increase in overall performance. Figure 13 shows a similar cell run by the Jung et al 2005. with a Nafion 117 membrane and 2.5M methanol. Like before, performance increases with increasing temperature because of improved kinetics.

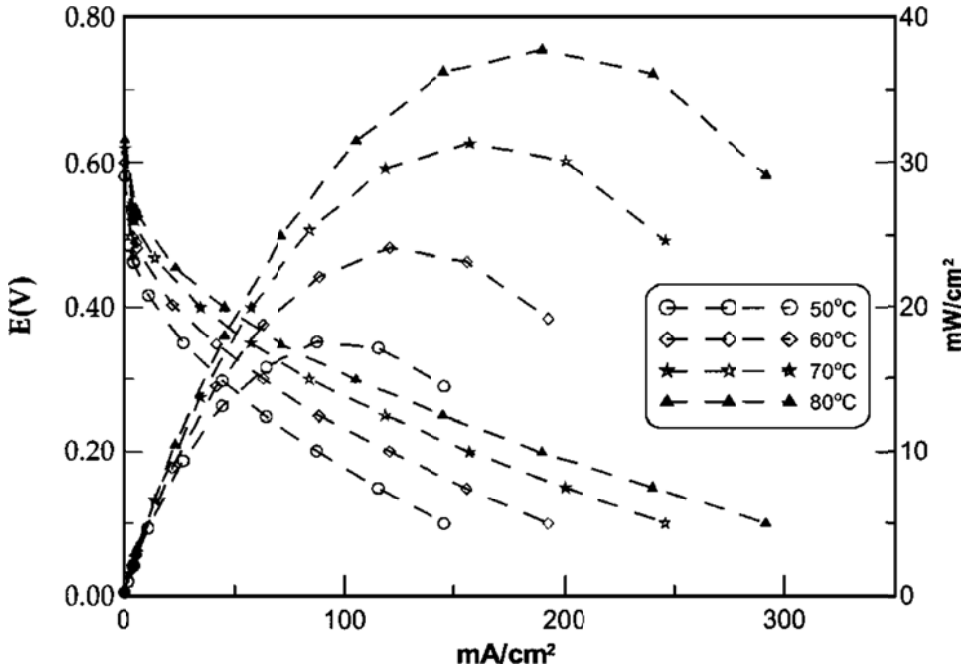

Figure 12: Various Operating Temperatures at 1M Runs (Jung et al., 2005)

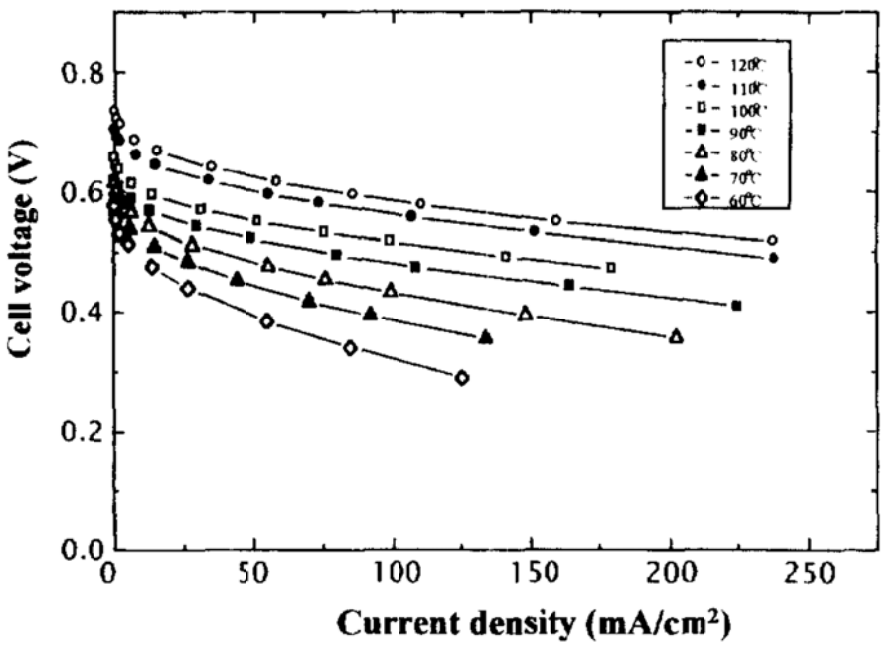

Figure 13: Various Operating Temperatures at 2.5M Runs (Jung et al., 1998)

Figure 14 shows the polarization plot of a Nafion 112 membrane with 3M methanol and its performance with increasing temperatures. Although performance does improve with increasing temperatures the 70ºC and 80ºC runs showed similar results.

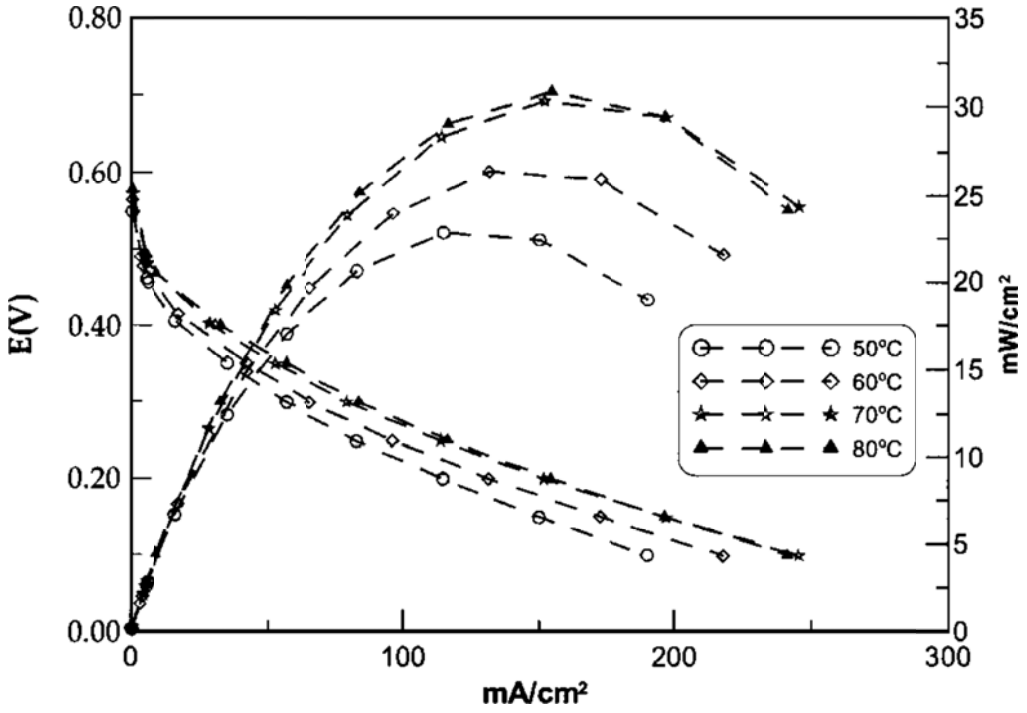

Figure 14: Various Operating Temperatures at 3M Runs (Jung et al., 2005)

Membrane thickness has an effect on the overall performance of the fuel cell. Figure 15 shows the performance of two membranes (Nafion 112 and 117) at 50^{o}C using 2M methanol. At higher current densities, the Nafion 112 membrane produced better results, but had a lower OCV when compared to the Nafion 117 membrane. This shows that the Nafion 117 has a higher resistance to methanol crossover but also reduces proton transport from the anode to cathode resulting in ohmic polarization (Jung et al.). Ohmic polarization (V=IR) is the loss of potential voltage in a fuel cell because of the resistance to the flow of ions in the electrolyte as well as the resistance of the flow of electrons through the cathode.

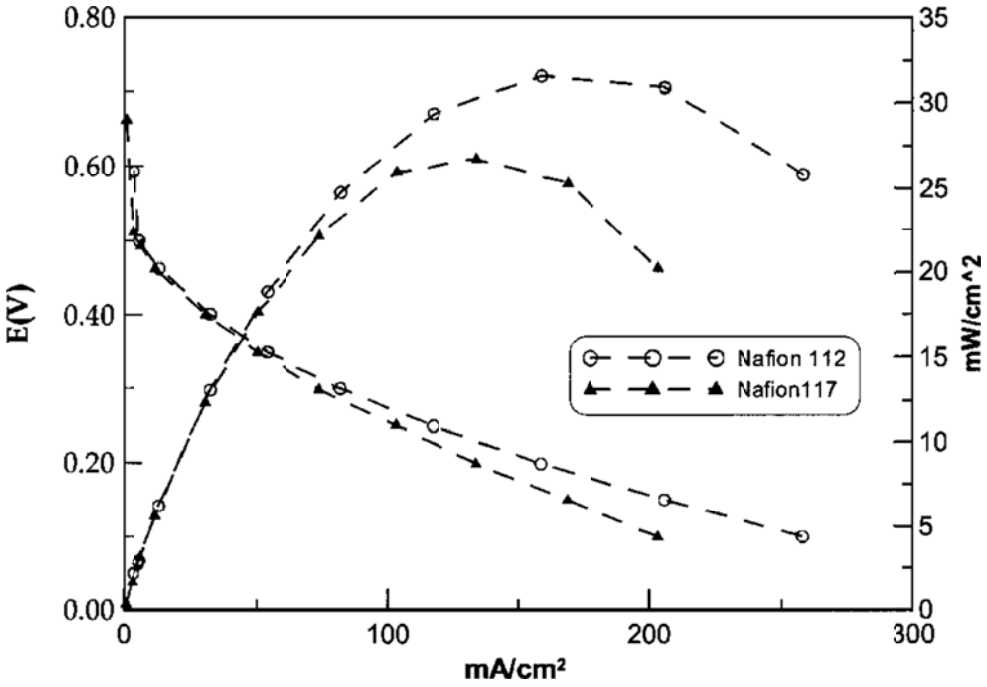

Figure 15: Nafion 112 and 117 Comparison at 50^{O}C and 2M (Jung et al., 2005)

Jung et al. showed similar results, as shown in Figure 16, under different parameters (Jung et al.). These results back up the fact that the fuel cell performance decreased with increasing membrane thickness at higher current densities. In addition, a thicker membrane also improves the OCV because it prevents methanol crossover.

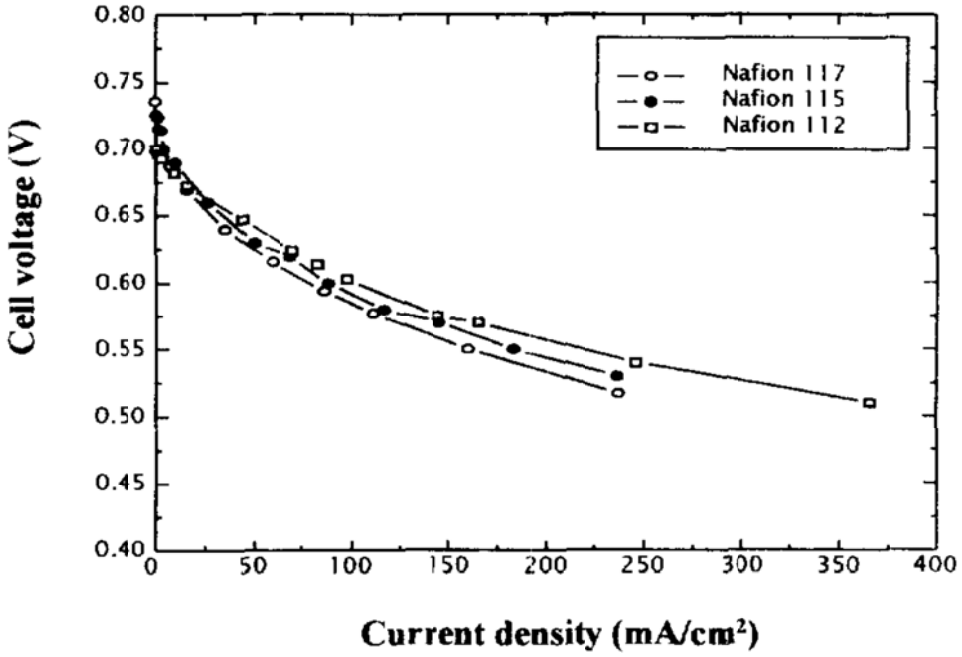

Figure 16: Nafion Membrane Comparison at 120^{O}C and 2.5M (Jung et al., 1998)

The flow rate of methanol also impacts the performance of a DMFC. Qi et al. analyzed the performance of varying flow rates using with a Nafion 112 membrane and 1M methanol using various temperatures. According to Figures 17-19 as the flow rate of methanol increased so did the overall performance. (Qi & Kaufman, 2002) Overall performance increased because there was a larger supply of methanol to react. Further, with an increase in temperature, the improvement between the flow rate increases became more significant. When comparing Figures 17 and 18, the performance of lower flow rates decreases with increasing temperature. Meanwhile at higher flow rates, there is slight increase in the performance with increasing temperature. The decrease in performance at lower flow rates is because the methanol that reacts isn't coming in at as fast of a rate as a higher flow rate as well as enhanced mass transfer at higher flow rates.

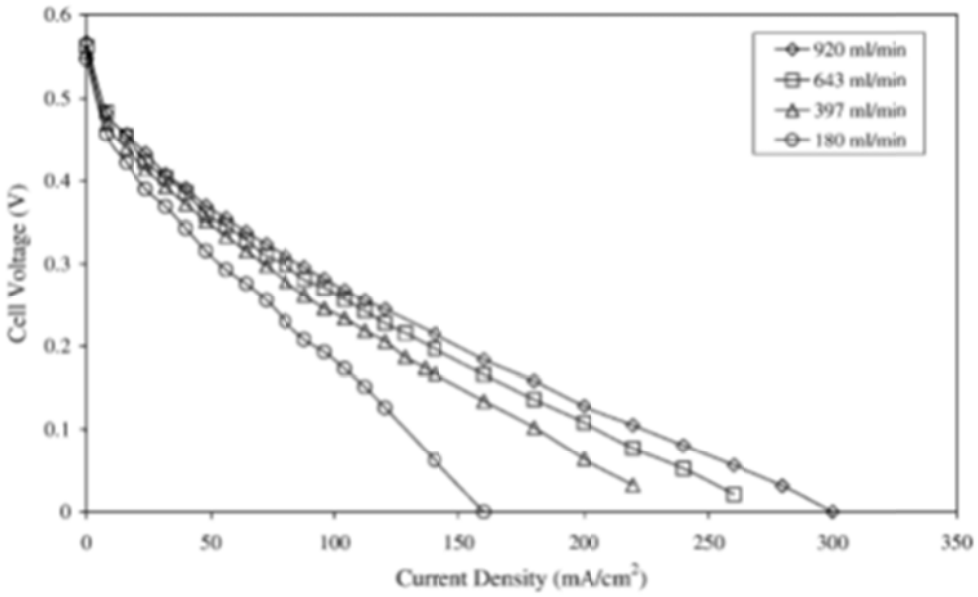

Figure 17: Various Flow Rates at 1M and 40^{O}C (Qi & Kaufman, 2002)

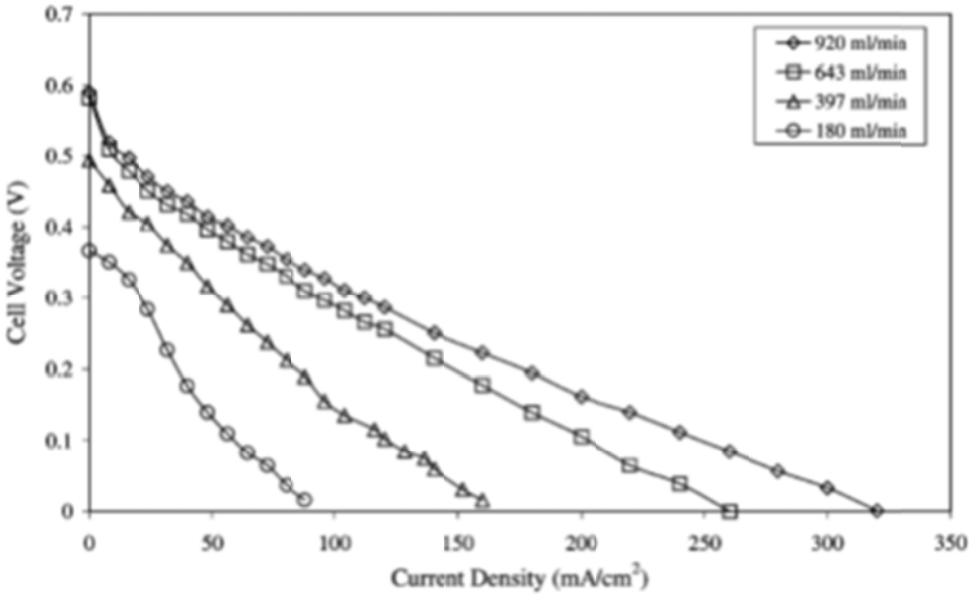

Figure 18: Various Flow Rates at 1M and 80^{O}C (Qi & Kaufman, 2002)

Methanol crossover is a major issue specific to DMFC and affects the overall performance of the fuel cell. This crossover not only wastes fuel but it can be electrochemically

oxidized at the cathode. (Qi & Kaufman, 2002) This oxidation can lower the cathode potential and consume some of the cathode reactant. Crossover can degrade the cathode from too much poisoning, which will result in lower performance and decreased efficiency.

As discussed, there are several operating parameters that are influential on DMFC performance. Combinations of various parameters can work well together, depending on the conditions in which they are operated. One of the biggest problems of concern is methanol crossover. However, reducing methanol crossover can be made possible by optimizing these various parameters. The fact of the matter is that getting the right combination of various operating parameters requires extensive experimental testing and analysis.

PBI Based MEAs

Polybenzimidazole (PBI) is of major interest in fuel cell technology because it can withstand operation at much higher temperatures than Nafion membranes. Increasing the temperature of a fuel cell is desirable for maximizing the power output; PBI membranes operate at temperatures in excess of $100^{o}C$ with a vaporized feed (Wainright et al, 1995).

Advantages of PBI over Nafion membranes include thermal stability, reduced water management and lower permeability to methanol. The two membranes conduct protons differently which is a result of their chemistry. Nafion requires liquid water to be present for proton transport by vehicle transport and Grotthus mechanism whereas PBI exhibits proton transport via the Grotthus mechanism (Chen et al, 2005).

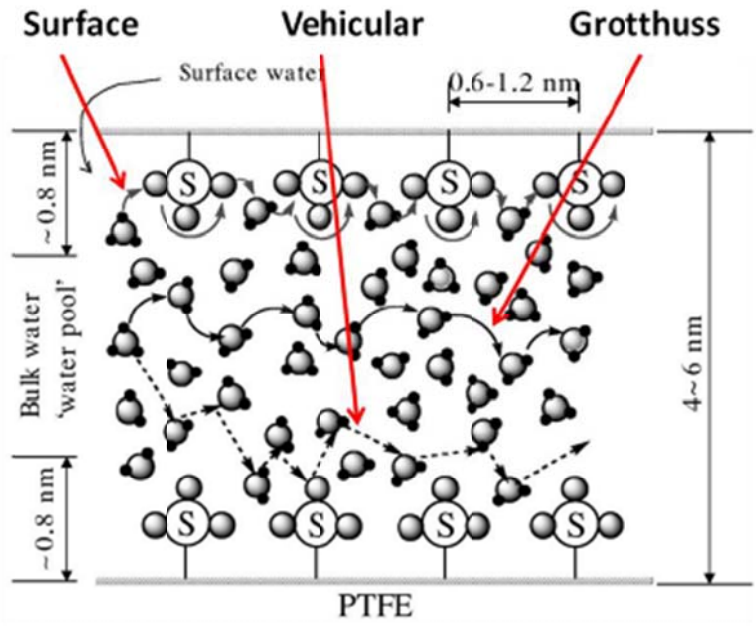

Figure 19: Proton Transport Mechanisms (Choi et al, 2005)

The Grotthus, or "proton-hopping," mechanism refers to covalent bonds being broken and reformed as the proton "hops" along the PBI molecule (Cukierman et al, 2006). Figure 20 displays a single mer of the PBI chemical make-up. Nafion contains C-C single bonds whereas PBI contains both phenyl and imidazole rings accounting for the far superior thermal stability.

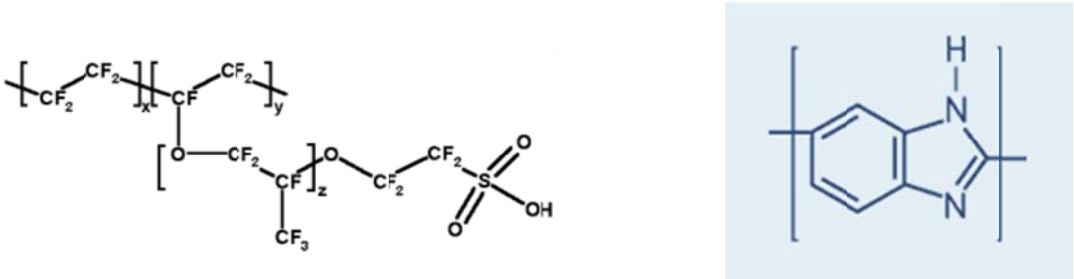

Figure 20: Mer structure for Nafion (left) (Dyck A., 2002) and PBI (right) (Polymer Chemistry 2010)

H_3PO_4

PBI membranes are doped with an electrolyte because alone PBI's conductivity is limited (Pu et al, 2004). The electrolyte serves to allow PBI the ability to conduct protons via the Grotthus mechanism and is usually phosphoric acid.

For every one molecule of PBI, retention of 2 H_3PO_4 is possible corresponding to the number of imidazole bonding sites (Lobato et al, 2006). Literature uses the term 'acid doping' or 'acid content' followed by an integer; this refers to the ratio of H_3PO_4 to PBI molecules. Researchers have studied the ratio of H_3PO_4 to PBI in order to maximize the conductivity of the PBI membrane.

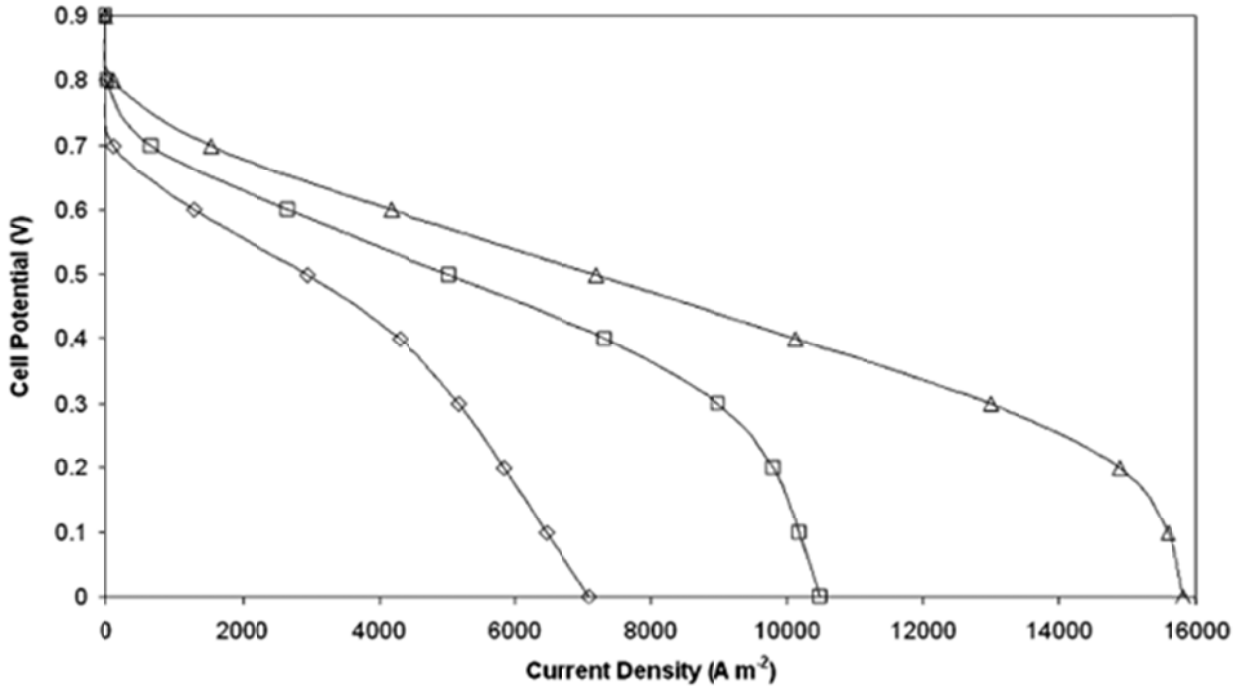

Figure 21: Polarization curve for PBI-H_3PO_4 for various acid doping; diamond (4.5) square (6.2) triangle (8) (Cheddie et al, 2006)

An increase in the amount of H_3PO_4 effectively improves the conductivity of the PBI membrane (Cheddie et al, 2006). Figure 21 shows polarization curves for three different MEA systems identical in thickness and catalyst loading but with different amounts of H_3PO_4. It is apparent that more H_3PO_4 gives a higher limiting current density. Chemically, a PBI molecule should be able to hold onto two molecules of H_3PO_4. In this graph the acid dopings are 4.5, 6.2 and 8.0 molecules of H_3PO_4 per PBI. He et. al describes a 'swelling' of the membrane for acid dopings greater than 2 which lead researchers to believe H_3PO_4 can exist between PBI polymer chains. (He et al, 2001). H_3PO_4 located in these 'pockets' improves the proton conductivity but reduces the secondary bonding of PBI molecules. With respect to the acid bath used to impregnate PBI, Lobato et. al observed mechanical failure at concentrations of 15M H_3PO_4 and above (Lobato et al, 2010).

The Grotthus mechanism is often described along with reduced water management but research shows that PBI requires water in addition to H_3PO_4 for reasonable proton conductivity (Lobato et al, 2007). Lobato et. al tested the proton conductivity of PBI under the following conditions to prove the importance of water: "at 190^{o}C, for a PBI membrane with a doping level of 6.2, proton conductivity is 0.015 S/cm when equilibrated in room air and 0.039 S/cm when equilibrated in saturated air at 60^{o}C" (Lobato et al, 2006). As a result of this finding studies typically humidify the cathode feed to prevent PBI's self-dehydration and maintain the membrane's proton conductivity (Pu et al, 2004).

Properties of PBI

PBI membranes are hygroscopic which can cause electrolyte leaching when exposed to liquid water (Chen et al, 2005). Figure 22 demonstrates the significance of H_3PO_4 leaching.

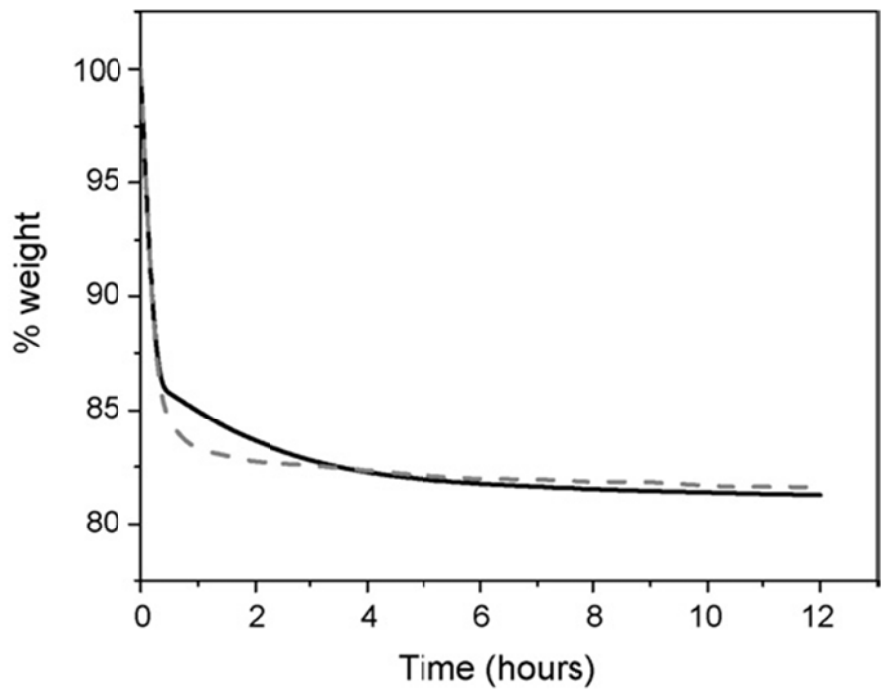

Figure 22: Relative change in weight of PBI-6.2 H_3PO_4 over time; solid line represents 150^{O}C and the dashed line 175^{O}C (Lobato et al, 2007)

During the first two hours of operation there is an approximate 16% weight loss in the PBI MEA (Lobato et al, 2007). As previously discussed, H_3PO_4 exists mostly between polymer chains. Water is being introduced through the anode feed and is being formed on the cathode electrode; in both instances H_3PO_4 can get leached out of the membrane and carried away.

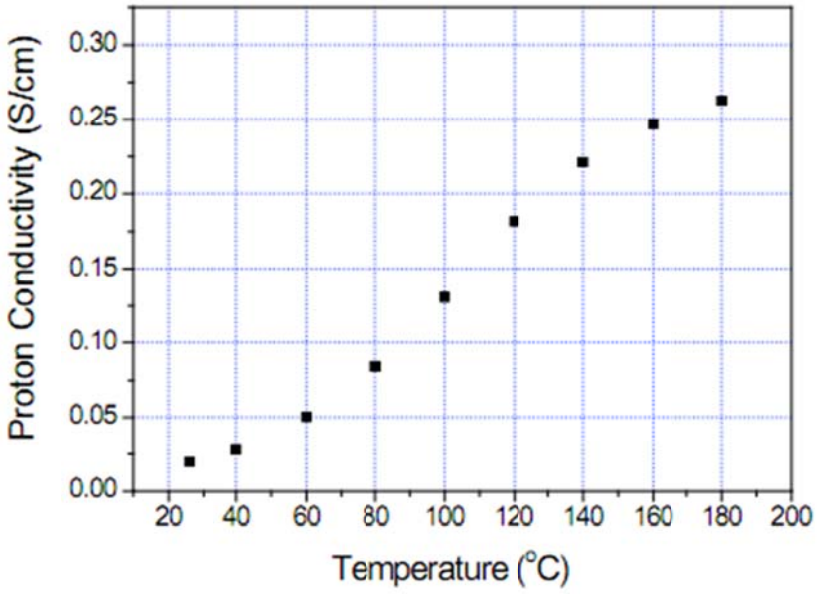

Figure 23: Proton conductivity of a PBI membrane with respect to temperature (Benicewicz, 2009)

Operating at a range of 120 – 200°C PBI membranes have potential to become prevalent in energy generation applications (Cheddie et al, 2006). As the temperature approaches 200°C the rate of conductivity improvement with temperature begins to decrease. The membrane remains thermally stable past 200°C but the improvement of kinetics is negligible to the cost of maintain the operating temperature.

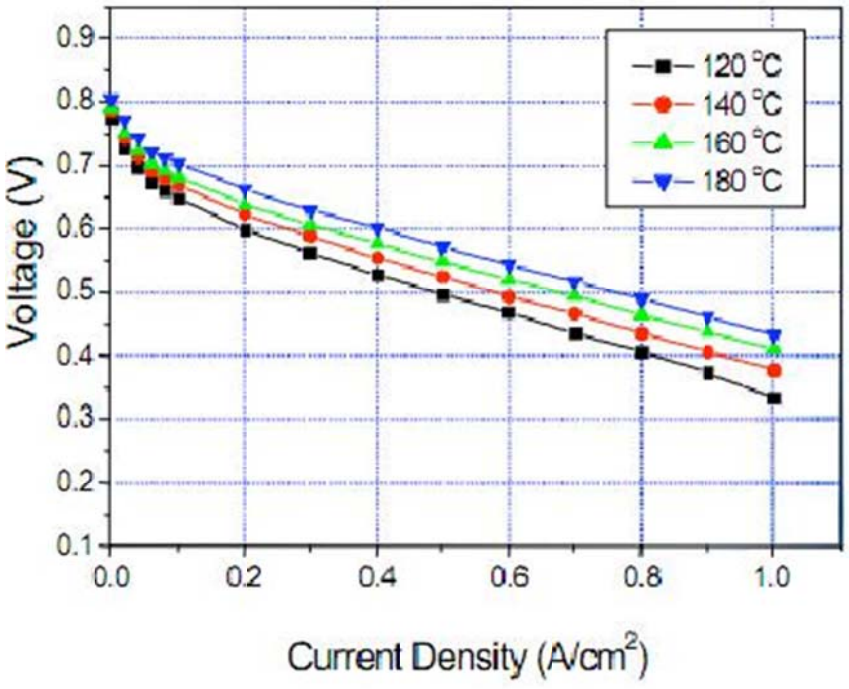

Figure 24: PBI polarization curve using a 2:1 stoichiometric ratio of H_2 to air (Benicewicz, 2009)

Jalani et. al theorize that the limiting current density for PBI- systems is improved with temperature due to mass transfer in the gas diffusion layer. At high temperatures, less water is formed on the porous GDL which allows for improved diffusion (Jalani et al, 2006).

In an analysis of PBI- H_3PO_4 systems, PBI with embedded H_3PO_4 and displayed a methanol permeability of 15 x 10^{-16} m^3 (STP)m/m^2 s Pa (Wainright et al, 1995). Wainright used a 2:1 water methanol solution but recent work suggests using a higher concentration of methanol in the feed. At concentrations in excess of 70% methanol, PBI permeability for methanol begins to decrease (Pu et al, 2004).

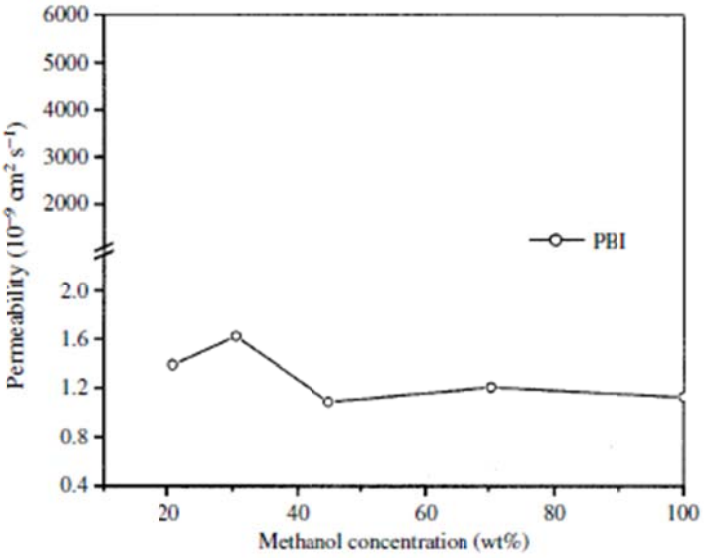

Figure 25: Permeability of methanol in PBI as a function of concentration (Pu et al, 2004)

Lobato et. al used multi-cycling sweep voltammetry to observe the effect of phosphoric levels on the electrode layer (Lobato et al, 2007). Over time the catalyst particles begin to agglomerate leading to a reduction in the active electrochemical surface area. Lobato observed that the agglomeration is more prevalent at higher temperatures allowing him to conclude that although temperature does improve performance it also causes a greater rate of degradation.

At high temperatures the embedded phosphoric acid can undergo a chemical transformation (J. Lobato, 2006).

$$2H_3PO_4 \rightarrow H_4P_2O_7 + H_2O \qquad < 2 >$$

Orthophosphoric, H_3PO_4, is desirable whereas pyrophosphoric acid, $H_4P_2O_7$, is far less conductive. This reaction does not occur often but evidently during long term operation of a PBI-H_3PO_4 system the performance diminishes as seen in Figure 26 (Benicewicz, 2009).

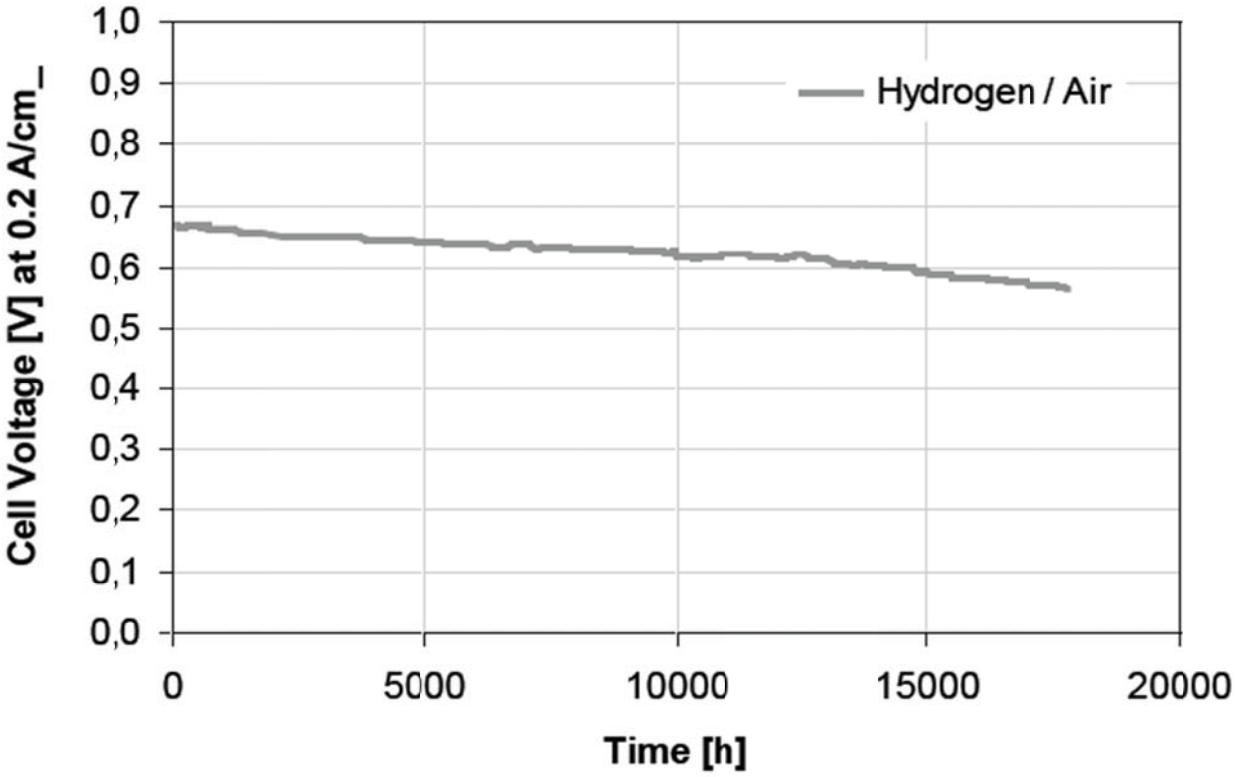

Figure 26: Durability polarization curve for a PBI membrane operated at 160^{O}C (Benicewicz, 2009)

Performance diminishes over time for three previously discussed reasons; the agglomeration of catalyst particles, conversion of orthophosphoric acid into pyrophosphoric acid and most importantly leeching of H_3PO_4 by water.

Chapter 3: Experimental

To test and measure the performance of a Nafion MEA in a DMFC, a conventional fuel cell station was used. Figure 27 shows a conventional fuel cell set up used for both Nafion and PBI MEAs. The methanol tank was used to feed the anode of the fuel cell while the ISCO Series D Pump Controller right below the tank was used to regulate the flow of the inlet. The temperature gauge and thermocouple was used to set the internal temperature of the fuel cell to the desired. The Tylan General RO-28 flow controller was used to regulate in the inlet flow of oxygen or hydrogen into the cathode and anode, respectively. The Hewlett Packard 6060 B System DC Electronic Load box was used to measure voltage and current of the fuel cell via an applied internal resistance.

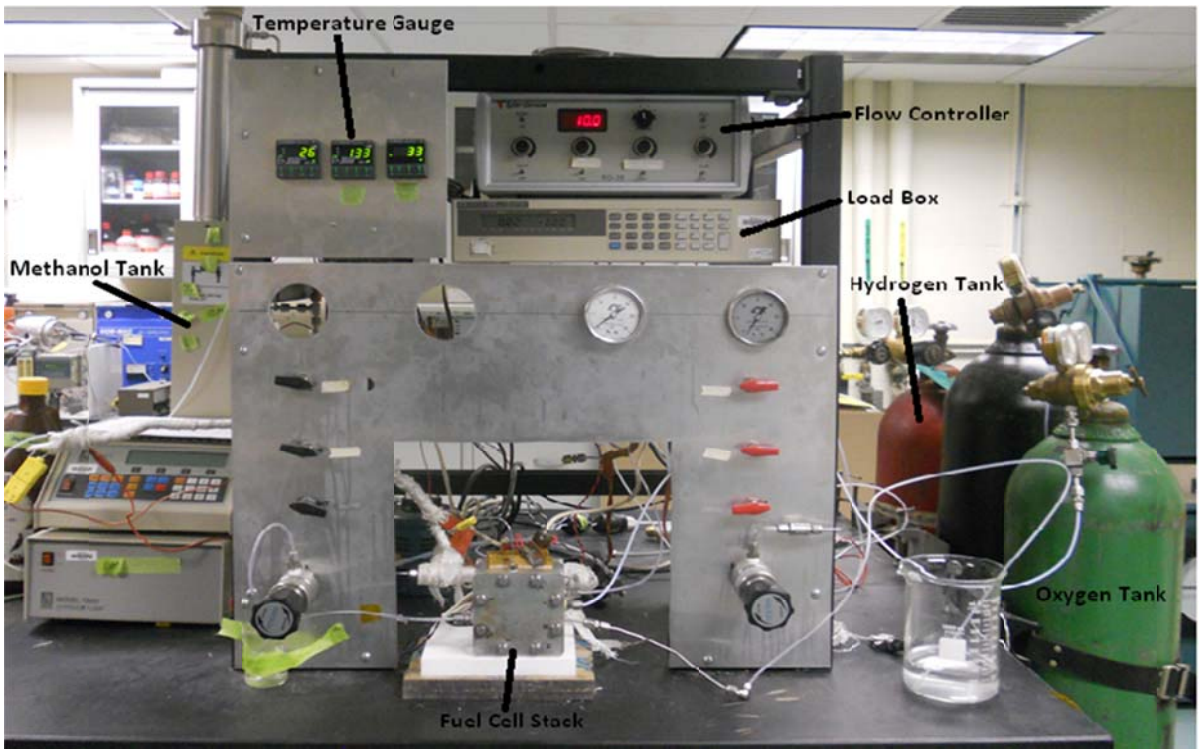

Figure 27: Fuel Cell Station Set up

The fuel cell stack in Figure 28 shows the side view of a fuel cell stack. It is very important when assembling the fuel cell stack to line up the gaskets and MEA directly over the serpentine pattern. When the gasket is placed on the anode bipolar plate, then the MEA is laid over that gasket, lining up the electrode over the flow channel minimizes leaks and poor contact with the fuel. After the MEA is lined up, a second gasket is placed over the MEA, followed by the cathode bipolar plate. This set up was used to test a commercial Nafion MEA from the fuel cell store under various parameters, including temperature, concentration and flow rate.

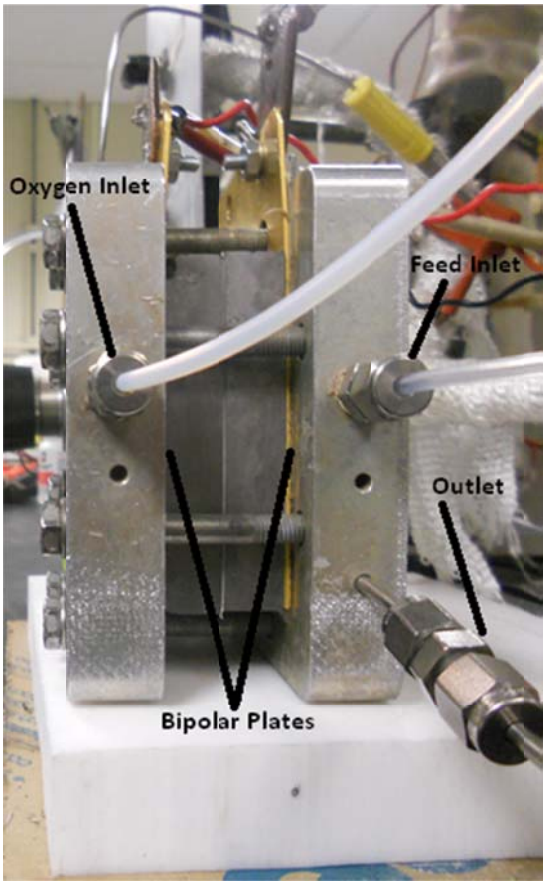

Figure 28: Side View of Fuel Stack

In order to run a PBI MEA in the setup being used, modifications were made to the fuel cell setup. While a Nafion MEA can run on a liquid feed, a PBI MEA requires a vapor feed due to its hygroscopicity. Therefore, the liquid methanol from the pump needed to be vaporized before entering the fuel stack. Further, the heat would cause the plastic tubing used for the inlet feed to melt. This plastic piping was replaced with metal piping. The metal piping was long enough to ensure the methanol would vaporize before reaching the fuel cell stack. To prevent heat loss, heating tape was wrapped around the metal piping and then was covered with a cloth wrap for insulation. The heating tape temperature was set by a control box and monitored by a temperature gauge. The PBI MEA that was used was purchased from BASF and was commercially made. There was no further prep work that needed to be done to the MEA as it was already good to be used in testing. Lastly, the gaskets being used in the fuel cell stack needed to be able to withstand temperatures ranging well over 100 ºC. These gaskets also need to be of the proper thickness as to ensure the electrode of the MEA was in proper contact with the feed in the flow channel of the bipolar plates.

Chapter 4: Results

Nafion Based MEAs

Nafion membranes, typically used in a DMFC were tested extensively under various parameters. The purpose of these experiments was to better understand how a fuel cell operates. The parameters tested where: the fuel cell temperature, the concentration of the methanol liquid feed and the flow rate. These runs used commercially produced MEAs to ensure high accuracy results.

The first parameter that was tested was temperature. Since a Nafion membrane is unstable at temperatures ranging above 100ºC the temperatures tested here were 25ºC, 50ºC, 70ºC and 90 ºC. Temperatures exceeding 100ºC decrease the performance of the fuel cell because the Nafion MEA will degrade. Figure 29 shows four runs done at four different temperatures with a constant flow rate of 1 ml/min and a 1M liquid methanol feed. These results show that overall performance increases as fuel cell temperature increases because as the temperature increases the rate of reaction increases causing there to be a higher current output. Figure 30 consists of three runs at various temperatures but with a change in its feed concentration (3M). However, the figure still shows the increased performance as the temperature is increased. Between the polarization plots shown in Figure 29and Figure 30, there is a clear difference in performance; the 3M runs have a much higher current density than the 1M runs, which indicates increased performance with increased concentration. At higher temperatures the amount of crossover at higher current densities is minimal as the temperature helps to increase proton conductivity and there increases the overall performance of the fuel cell.

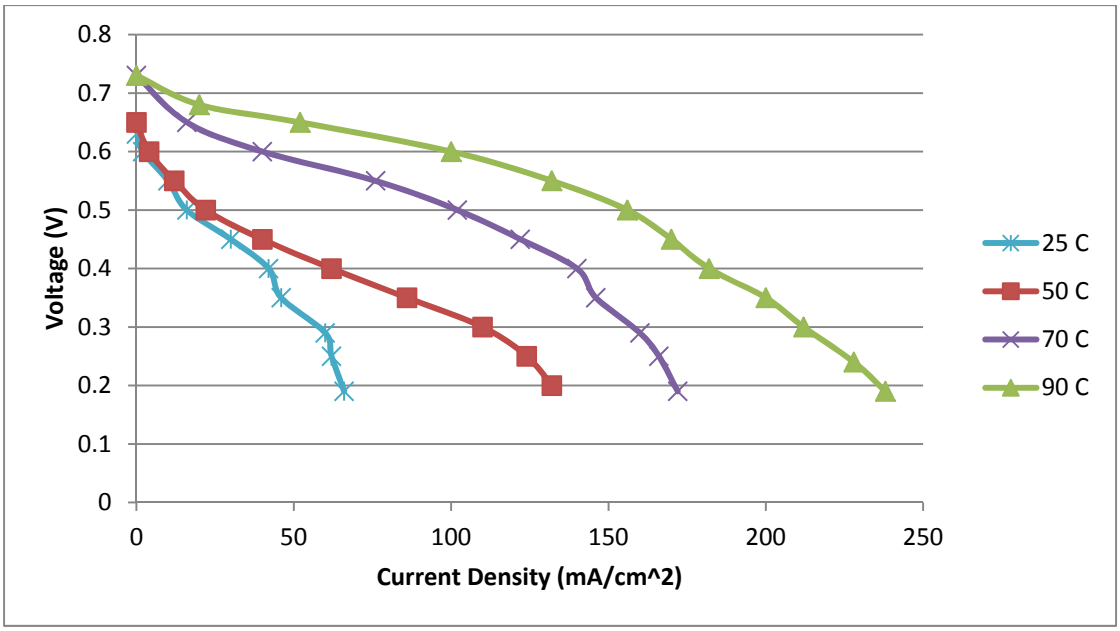

Figure 29: Temperature Variation (1M)

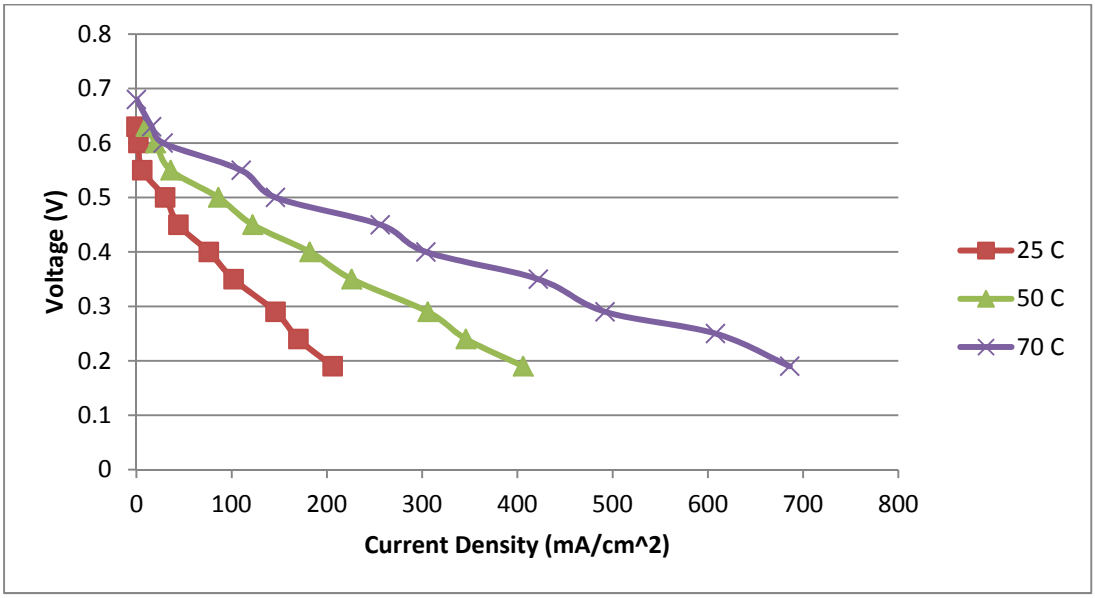

Figure 30: Temperature Variation (3M)

Next, the concentration of the methanol liquid feed was changed to measure the overall performance of the fuel cell. 1M and 3M liquid methanol were tested at 70ºC with a flow rate of 1 ml/min. Figure 31 shows the results of three 3M runs and two 1M runs. The results show that

voltage increases with concentration at higher current densities because the methanol concentration is greater and therefore creates more proton conductivity. Another important observation is the OCV; the OCV using 1M MeOH is higher than 3M MeOH. This lower OCV is due to increased methanol crossover. Methanol crossover increases with concentration, however, at higher current densities the more methanol is needed to react. This explains why the performance is better at higher concentrations because there is more methanol to continue to react with the electrode. Although the results are not consistent with each other and there was different performance for the same concentrations and performance is increased with methanol concentration to a certain degree. Too high a concentration at these lower temperatures (<100ºC) will results in significant crossover and an extremely low OCV that will result in poor performance. A lower concentration of methanol (<1M) will result in a higher OCV but the overall performance will decrease because there will not be as much methanol to react as current density is increased.

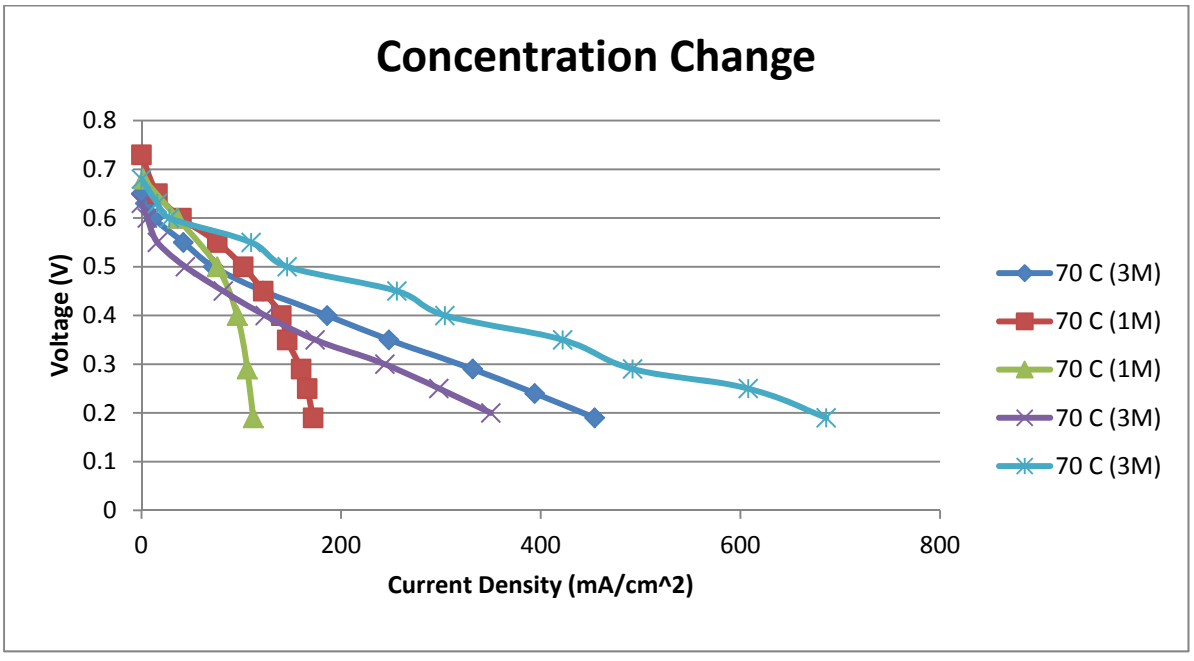

Figure 31: Concentration Variation (1M & 3M)

Because of the inconsistent results from Figure 32, the MEA's consistency was tested. An MEA was run several times under the following conditions: 70ºC, 3M MeOH and 2 mL/min. Figure 32 shows the results of 5 different runs over 15 hours. The results show reproducible results, which indicate that the MEA and fuel cell are performing consistently. The performance of an MEA over an extended period of time is subject to the conditions that it is run at. If a Nafion MEA is run for an extended period of time at high temperatures and high concentrations i.e. 90ºC and 3M then the lifetime of that MEA will be shortened and the performance will decrease with time.

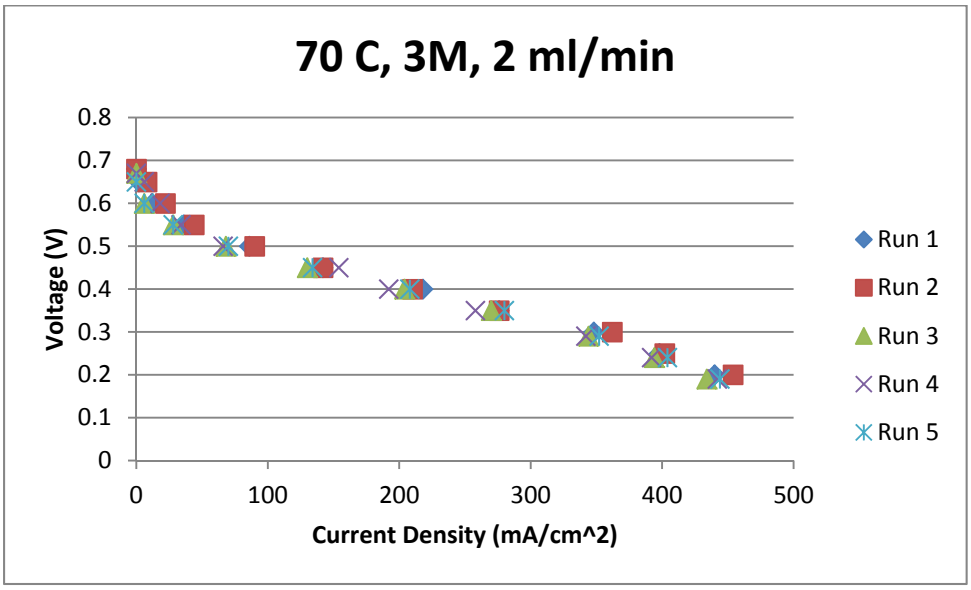

Figure 32: Consistency Run (70 C, 3M, 2 ml/min)

These Nafion MEA tests were done with the purpose of measuring performance under various parameters. These experiments gave good insight as to how sensitive a DMFC's performance is based on parameter changes. These informative results helped in the experimentation of PBI MEAs in the DMFC set up. Since PBI MEAs must be run at higher

temperatures and our data obtained indicates that overall should increase. However, methanol vaporizes at higher temperatures and so the concentration of methanol must be adjusted.

PBI Based MEAs

To extend the range of temperatures for DMFCs, PBI-based MEAs were tested Despite the high quality of the BASF PBI MEAs, they did not perform as well as expected. Vapor methanol achieved an OCV of 0.22V at 140^{o}C at a flow rate of 2.0 ml/min and concentration of 12M. An OCV of 0.44V was obtained using non-humidified oxygen and hydrogen at 150^{o}C. Again at 150^{o}C, an induced voltage of 0.10V output a current of 4.50A; this experiment was allowed to run for 60h and the current dropped to 3.90A.

Despite the good performance on a single occasion the PBI membranes failed to perform on a consistent basis. Systematic troubleshooting was performed to account for all of the reasons why high temperature PBI MEA lacked performance. The pressure at the anode was observed to reach elevated levels using vapor methanol. Additionally, OCV data suggested a short circuit when using hydrogen. Finally, the compressibility of the membranes was unknown until recently and the proper gasket material was not used.

In order to run the PBI membrane, the methanol feed needed to be vaporized to avoid loss of the electrolyte. The vaporized feed caused a fluctuation in the anodic pressure which was observed on the methanol pump. During standard operation the pump would reach a pressure of about 20 atm. Start up for vaporized methanol would show normal behavior but after equilibration had occurred and the destination temperature reached, the pressure of the pump would spike to values close to 60 atm. This fluctuation in pressure increased the methanol crossover occurring which is a very likely reason for the low 0.22V OCV. In order to address

this issue, the flow rate on the methanol pump was set to constant pressure; however, the inlet flow rate would fluctuate anywhere between 1and 18 ml/min. Too high a flow rate and proper vaporization of the feed is not achieved; when liquid reaches the MEA there is a good chance for desorption which permanently reduces the membranes effectiveness.

Fuel cell assembly is crucial in order to get performance. The bipolar plates are bolted together to a particular tightness. The tightness used for Nafion membranes is what was originally used for the PBI membranes; however after several unsuccessful runs the tightness of the bolts was tested. The bolts were loosened from ~65 lb_f-in and it was found that if the bolts were tightened past 45 lb_f-in, the performance of the cell would drop to 0.02 immediately. According to BASF engineer the proper torque of 6 N-m or ~62 ib_f-in was the right tightness of the bolts for the fuel cell stack. Unfortunately, this only helped the performance for a short period of time and eventually the OCV dropped down again.

The MEA must be properly aligned with the flow channels; the slightest error in assembling the fuel cell can result in gas leaks or short circuits. One membrane suffered what was initially a pinhole in the top left corner. This eventually turned into a large hole shown in Figure 33. This tear in the membrane allowed both oxygen and methanol to flow freely through the membrane, causing over potential at both cathode and anode electrodes. A tear of this magnitude renders the MEA useless because it is unable to serve as a fuel barrier. The fuel cell stack was frequently disassembled and inspected in order to assure the MEA was in proper functioning condition.

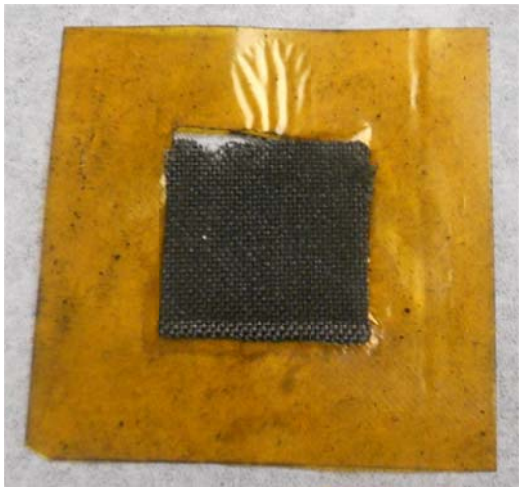

Figure 33: Torn PBI MEA

A Nafion MEA typically has a compression of around 20%, however, the PBI membrane purchased from BASF has a 50% compression. These values coincide with the reported observation about bolt tightness; higher compression rating requires a lower amount of applied torque. Operating PBI membranes at a higher than required torque would result in a higher methanol flux, thereby increasing the rate of acid desorption.

Inside the fuel stack, gaskets are inserted between the bipolar plates and the MEA. It is important that the gasket material is adequate for the fuel cell's operating temperature. It is imperative that the membrane be made out of a material that has a melting point higher than the operating temperature.

Gasket thickness is also important for successful DMFC operation. The thickness of the gasket is proportional to the thickness of each side of the electrode assembly. The purchased BASF PBI MEAs had an overall MEA thickness of 0.98mm with each electrode accounting for 0.44 mm. In Appendix V, there is a table given by BASF to measure gasket thickness based on the compression of the MEA and the thickness of each electrode.

PBI-H_3PO_4 is prone to acid desorption which was observed in the lab. Firstly, the experiment done at 0.1V showed an initial current of 4.5A and then 60 hours later a current of 3.90A. The MEA was fresh in the sense it had not been used prior to that experiment. The drop in current is due mostly to acid desorption. Additionally, experiments done with non-humidified hydrogen oxygen showed diminishing OCV after repeated experiments. One PBI MEA that had gone from 0.44V to 0.02V several runs later was administered an acid treatment; several drops were placed around the electrode assembly on each anode and cathode side of the membrane and given a day to sorb in. The MEA was run under the same conditions with hydrogen and showed improvement of OCV back up to 0.42V. Interestingly, after only an hour the OCV had already dropped back to 0.02V. It is probable that H_3PO_4 had only been deposited on the surface of the membrane where it is most prone to desorption. The remediated OCV showed that the acid treatment works but the rapid drop in OCV proves the unreliability of re-treating PBI membranes with H_3PO_4.

Chapter 5: Conclusions

Nafion Based MEAs

After analyzing the data taken under this study it can be concluded that as the concentration of the inlet feed of liquid methanol increased, the performance of the Nafion MEA would also increase with the range of concentrations tested. It was observed that at low current densities, a lower concentration of methanol improved performance; this is due to methanol crossover being more prevalent at low current densities.

Polarization curves focused on the effect of changing temperature and keeping the feed concentration and flow rates constant. Over the temperature range of $25^{o}C$ to $90^{o}C$ Nafion membranes performed better with higher temperatures. Also, the limiting current density increased as temperature was increased.

PBI Based MEAs

Polarization curves could not be obtained for PBI based MEAs due to time limitations. The PBI-H_3PO_4 MEA was used with both vaporized methanol and hydrogen in the DMFC with little success; an OCV of 0.44V was obtained for non-humidified hydrogen at $150^{o}C$ and an OCV of 0.22V for vapor methanol at $140^{o}C$. A current of 4.50A was obtained at a voltage of 0.1V at a temperature of $150^{o}C$ using a fresh PBI MEA. This membrane was permitted an uninterrupted 60 hour operation after which the current was 3.90A.

The pressure of the anode feed was observed to be extremely high for DMFC PBI operation at $140^{o}C$ and above resulting in excessive methanol crossover and no performance.

The compression of the BASF PBI membrane was higher than expected, 50%, and many of the failed runs were attempted at too high a torque between the bipolar plates Additionally, the gasket material used was not ideal for PBI operation because it ran the risk of melting and was not of perfect thickness. Lastly, H_3PO_4 desorption was observed as the OCV dropped from 0.44V to 0.02V. An acid treatment was administered and the resultant OCV was remediated but only for a short time.

Overall, the effect of temperature on performance was observed through use of Nafion membranes and literature review. Concentration of methanol in the feed was also varied and comparison of polarization curves showed signs of methanol crossover. PBI membranes did not give consistent data but did show promise for large current density at intermediate temperatures.

Chapter 6: Recommendations

Although we were unsuccessful in producing polarization curves for PBI-H_3PO_4 there are several points that should be considered that might enable consistent performance. Firstly and most importantly, a gasket material specific to the electrode thickness should be used that can withstand operation up to 200^0C. BASF sells specific gaskets depending on thickness and compressibility of the membrane. Secondly and related to the first point is the amount of torque applied to the bipolar plates. The tightness of the bolts was shown to directly affect whether or not current could be obtained from the system; too high a torque and short circuiting occurred and too loose leakage will occur. We recommend using a torque of 40, 45 lb_f-in to get the best results.

Consideration should be placed on how the MEA is 'broken in.' Lobato et. al showed performance as a function of the 24h break in temperature; at high temperatures new MEAs loose water and acid content much quicker at more moderate temperatures (J. Lobato, 2006). Desorption of H_3PO_4 can be reduced by breaking the MEA in at 100-120^{o}C before turning up the temperature to a desirable operating value.

After running a MEA for several days' worth of experiments diminished performance should be expected; use of a 10M H_3PO_4 bath was shown to temporarily produce remediated OCV levels. It is likely that the longer the MEA is allowed to soak in the acid bath, the greater the retention rate of H_3PO_4. There are two ways to go about testing the MEA for H_3PO_4 retention; observe how long it takes for the OCV to decrease by a certain value or weigh the MEA after an amount of time and compare to the starting weight (Lobato, Canizares, Rodrigo, & Linares, 2007).

Lastly, we recommend frequent disassembly and inspection of the MEA and flow channels. Small bits of carbon cloth were observed to ‘clog’ up the small flow channels and had to be removed. The MEA can form small pinholes that are difficult to detect with the naked eye; inspecting the outer perimeter of the electrode assembly for any damage or wear should be a habit every time the fuel assembly is reconstructed.

References

FC2K. (2000). Retrieved November 10, 2010, from Fuel Cell Basics: http://fuelcells.org/

Toshiba's methanol fuel cell. (2004, June 24). Retrieved from DP Review: http://www.dpreview.com/news/0406/04062401toshibafuel.asp

A Basic Overview of Fuel Cell Technology. (2008). Retrieved from American History: http://americanhistory.si.edu/fuelcells/basics.htm

DOE- Fossil Energy: Office of Fossil Energy Home Page. (2010, April 23). Retrieved 16 2010, November, from DOE- Fossil Energy: DOE's Fuel Cell R&D Program: http://www.fossil.energy.gov/programs/powersystems/fuelcells/

Fuel Cell Store. (2011). Retrieved from http://www.fuelcellstore.com/

A. Heinzel, V. B. (1999, June 22). A review of the state-of-the-art of the methanol crossover in direct methanol fuel cells. Freiburg, Germany.

Benicewicz, B. C. (2009). High Temperature PBI membranes. South Carolina: University of South Carolina.

Chen, K., Hickner, M., & and Noble, D. (2005). Simplified models for predicting the onset of liquid water droplet instability at the gas diffusion layer/ gas flow channel interface. *Internation journal of Heat and Mass Transfer 29*, 1113-1130.

Choi Pyoungho, J. N. (2005). Thermodynamics and Proton Transport in Nafion - Proton Diffusion Mechanisms and Conductivity . *Journal of The Electrochemical Society Vol. 152*, 123-130.

Cukierman, S. (2006). Et. tu. Grotthuss! and other unfinished stories. *Biochim Biophys Acta*, 876-885.

Denver F. Cheddie, N. D. (2006, December 12). A two-phase model of an intermediate temperature PEM fuel cell. Miami, Florida, USA.

Dyck A., F. D. (2002). Proton-conductive membranes of sulfonated polyphenylsulfone. *Journal for Applied Polymer Science*.

FCTec Home Page. (n.d.). Retrieved November 10, 2010, from http://www.fctec.com/index.asp

Garcia, B. L. (2004). Methanol Model of a Direct Methanol Fuel Cell. *Journal of Fuel Cell Science and Technology*, 43-48.

Hackguard, A. (2005). *Improving and Understanding Direct Methanol Fuel Cell Performance.* Worcester: Worcester Polytechnic Institute.

Hai, S. e. (2005). Pd Electroless Plated Nafion Membrane For High Concentration DMFCs. *Journal of Membrane Science 259*, 27-33.

Han-Kyu Lee, J.-H. P.-Y.-H. (2003). A study on the characteristics of the diffusion layer thickness and the porosity of the PEMFC. *Journal of Power Sources*, 131: 200-206.

J. Lobato, P. C. (2006, March 3). Synthesis and characterisation of poly[2,2-(m-phenylene)-5,5-bibenzimidazole] as polymer. Ciudad Real, Spain.

J. S. Wainright, J.-T. W. (1995). Acid-Doped Polybenzimidazoles:A New Polymer Electrolyte. Cleveland, Ohio, USA.

Jin Hu, V. B. (2008). PEO-PPO-PEO triblock copolymer/Nafion blend as membrane material for intermediate temperatre DMFCs. *J Appl Electrochem*, 38: 543 - 550.

Jung, D., L.H., C., & Chang, S. D. (1998). Performance of a Direct Methanol Polymer Electrolyte Fuel Cell. *Journal of Power Sources 71*, 169-173.

Jung, G., Su, A., Tu, C., & Weng, F. (2005). Effect of Operating Parameters on the DMFC Performance. *Journal of Fuel Cell Science and Technology 2.2*, 81-92.

Justo Lobato, P. C. (2010). Study of the influence of the amount of PBI–H3PO4 in the catalytic layer of a high temperature PEMFC. Camilo Jose Cela, Ciudad Real, Spain.

Lobato, J., Canizares, P., Rodrigo, M. A., & Linares, J. J. (2007). PBI-based polymer electrolyte membrane fuel cells: temperature effects on cell performance and catalyst stability. *Electrochimica Acta 52*, 3910-3920.

Lobato, J., P., C., Rodrigo, M., & Linares, J. (2009). Testing a vapour-fed PBI-based Direct Ethanol Fuel Cell. *Fuel Cells*, 597-604.

Nikhil H. Jalani, M. R. (2006, May 3). Performance analysis and impedance spectral signatures of high temperature PBI–phosphoric acid gel membrane fuel cells. *Journal of Power Sources*, 1096-1103.

Pivovar, B. S. (2006). An overview of electro-osmosis in fuel cell polymer electrolytes. *Polymer*, 4194-4202.

Prasanna, M., Ha, H., Cho, E., Hong, S., & Oh, I. (2004). Investigation of oxygen gain in polymer electrolyte membrane fuel cells. *Journal of Power Sources 137*, 1-8.

Pu, H., & Liu, O. (2004). Methanol permeability and proton conductivity of polybenzimidazole and sulfonated polybenzimidazole. *Polymer International 53*, 1512-1516.

Qi, Z., & Kaufman, A. (2002). Open Circuit Voltage and Methanol Crossover in DMFCs. *Journal of Power Sources 110*, 177-185.

R. He, Q. L. (2001). Physiochemical properties of phosphoric acid doped polybenzimidazole membranes for fuel cells. *Journal of Membrane Science*, 38-45.

S.A. Vilekar, R. D. (2010). The Effect of Hydrogen Crossover on Open-Circuit Voltage (OCV) in PEM Fuel Cells. *Journal of Power Sources*, 2241-2247.

Springer, T., Zawodzinski, T., & Gottesfeld, S. (n.d.). Polymer Electrolyte fuel cell model. *Journal Of electrochemical science 138*, 2334-2342.

Steinkamp, Schumacher, Goldsmith, Ohlberger, & Ziegler, J. (2008). A non-isothermal PEM fuel cell model including two water transport mechanisms in the membrane. *Fuel Cell Science Technology*, 1-26.

Transforming the Energy Network. (n.d.). Retrieved from Fuel Cell & Hydrogen Energy Association: http://www.fchea.org/

USFCC. (n.d.). Retrieved November 7, 2010, from About Fuel Cells: http://www.usfcc.com/index2.html

Wainright, J. S., Wang, J.-t., & Saviinell, R. F. (1996). Direct Methanol Fuel Cells Using Acid Doped Polybenzimidazole as a Polymer Electrolyte.

Acknowledgements

We would like to thank the following people for helping us with this project over the course of this academic year:

-Professor Datta for giving us the privilege to work on an exciting project, expanding our knowledge about fuel cells, and motivating us to accomplish our goals.

-Neal Rosenthal for his constant support and providing information during our time working on this project. He was more than willing to answer any questions that we had and suggesting new ways and directions to attack our problems and accomplish our goals.

-Jack Ferraro and Doug White for helping with any issues that would arise from working with our fuel cell station set up. They always were able to pinpoint a problem and help us fix it.

-Dan Knox for his support during this project and helping us by allowing us to use his equipment.

Appendices

Appendix I: Self-Made MEAs Andrew and Bob

Andrew									
	Run 1	1 ml/min	70 C	1 Molar		Run 2	1 ml/min	70 C	1 Molar
		Voltage	Cdensity				Voltage	Current	CDensity
		0.2	96				0.2	0.26	52
		0.3	70				0.3	0.11	22
		0.4	16				0.4	0.01	2
		0.5	2				0.5	0	0
		0.53	0				0.49	0	0

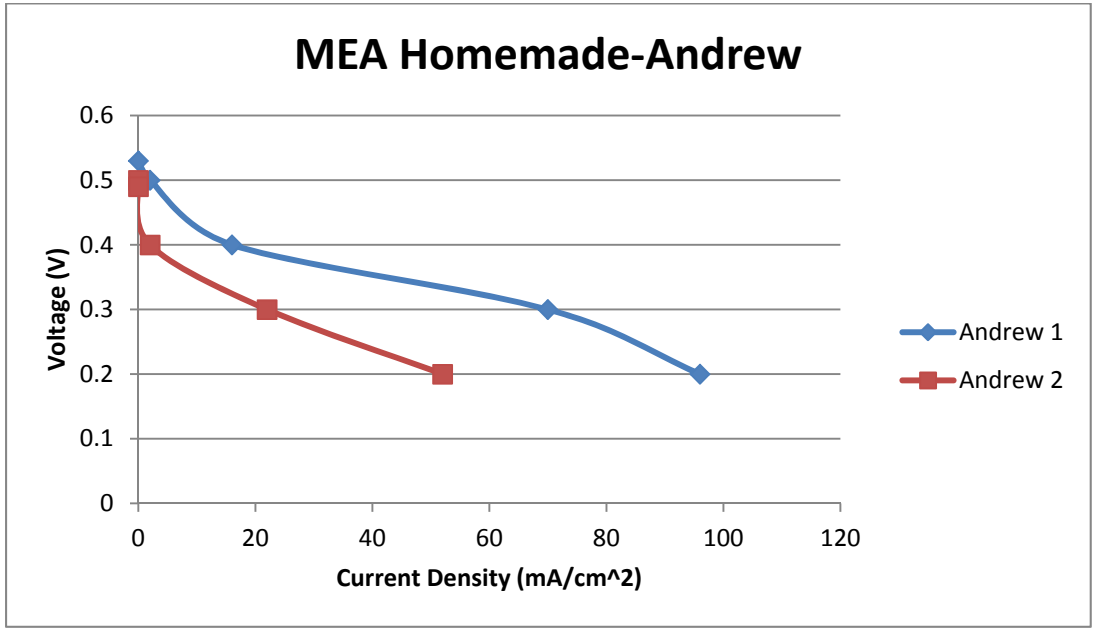

Bob														
	Run 1	1 ml/min	70 C	1 Molar		Run 2	2 ml/min	70 C	1 Molar		Run 3	2 ml/min	70 C	1 Molar
		voltage	current	cDensity			voltage	current	Cdensity			voltage	current	cdensity
		0.2	0.48	96			0.2	0.51	102			0.19	0.42	84
		0.25	0.36	72			0.25	0.4	80			0.24	0.35	70
		0.3	0.25	50			0.3	0.28	56			0.29	0.21	42
		0.35	0.13	26			0.35	0.15	30			0.35	0.13	26
		0.4	0.06	12			0.4	0.08	16			0.39	0	0
		0.45	0.01	2			0.45	0.05	10					
		0.5	0	0			0.57	0	0					
		0.52	0	0										

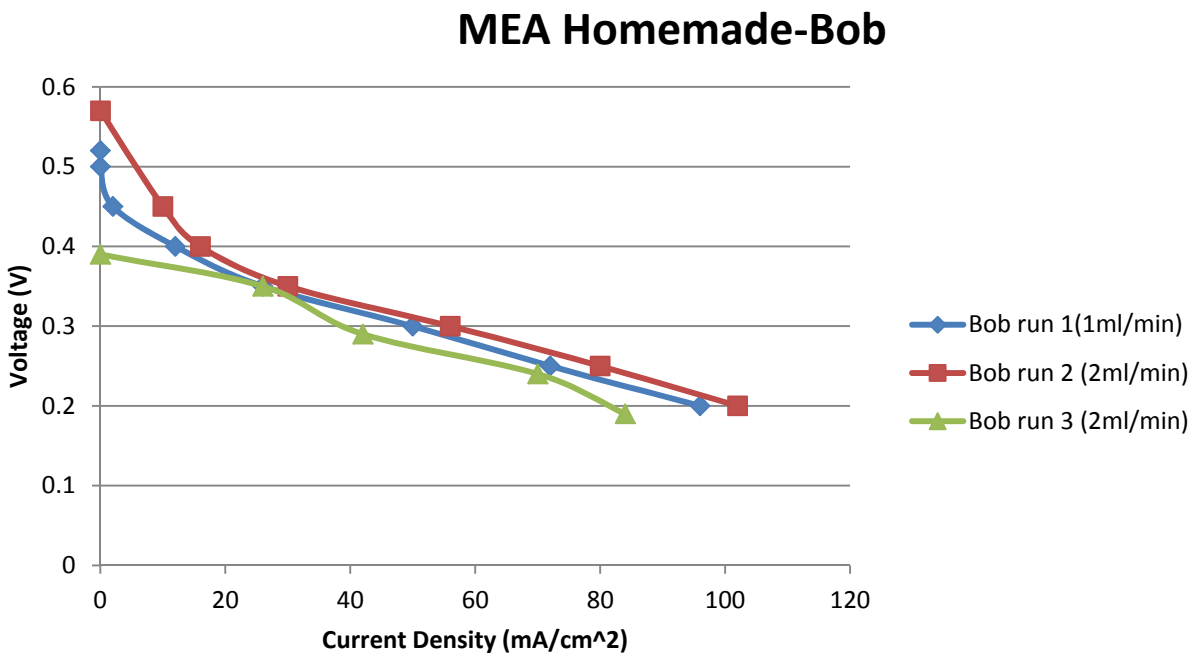

Appendix II: Commercial MEA Experimental Runs and Results

Run 1	1 ml/min	70 C	1 Molar		Run 2	1 ml/min	50 C	1 Molar		Run 3	1 ml/min	90 C	1 Molar
11/2/2010	Voltage	Current	Cdensity		11/4/2010	Voltage	Current	Cdensity		11/8/2010	Voltage	Current	Cdensity
	0.19	0.56	112			0.2	0.66	132			0.19	1.19	238
	0.29	0.53	106			0.25	0.62	124			0.24	1.14	228
	0.4	0.48	96			0.3	0.55	110			0.3	1.06	212
	0.5	0.38	76			0.35	0.43	86			0.35	1	200
	0.6	0.18	36			0.4	0.31	62			0.4	0.91	182
	0.68	0.01	2			0.45	0.2	40			0.45	0.85	170
						0.5	0.11	22			0.5	0.78	156
						0.55	0.06	12			0.55	0.66	132
						0.6	0.02	4			0.6	0.5	100
						0.65	0	0			0.65	0.26	52
											0.68	0.1	20

Run 4	1 ml/min	70 C	1 Molar		Run 5	1 ml/min	25 C	1 Molar		Run 6	1 ml/min	70 C	3 Molar
11/9/2010	Voltage	Current	Cdensity		11/10/2010	Voltage	Current	Cdensity		11/11/2010	Voltage	Current	Cdensity
	0.19	0.86	172			0.19	0.33	66			0.19	2.27	454
	0.25	0.83	166			0.25	0.31	62			0.24	1.97	394
	0.29	0.8	160			0.29	0.3	60			0.29	1.66	332
	0.35	0.73	146			0.35	0.23	46			0.35	1.24	248
	0.4	0.7	140			0.4	0.21	42			0.4	0.93	186
	0.45	0.61	122			0.45	0.15	30			0.45	0.61	122
	0.5	0.51	102			0.5	0.08	16			0.5	0.36	72
	0.55	0.38	76			0.55	0.05	10			0.55	0.21	42
	0.6	0.2	40			0.6	0.01	2			0.6	0.06	12
	0.65	0.08	16			0.63	0	0			0.63	0.02	4
	0.73	0	0										
											0.73	0	0

Run 7	1 ml/min	70 C	3 Molar		Run 8	1 ml/min	70 C	3 Molar		Run 9	1 ml/min	50 C	3 Molar
11/15/2010	Voltage	Current	Cdensity		11/16/2010	Voltage	Current	Cdensity		11/18/2010	Voltage	Current	Cdensity
	0.2	1.75	350			0.19	3.43	686			0.19	2.03	406
	0.25	1.49	298			0.25	3.04	608			0.24	1.73	346
	0.3	1.22	244			0.29	2.46	492			0.29	1.53	306
	0.35	0.87	174			0.35	2.11	422			0.35	1.13	226
	0.4	0.62	124			0.4	1.52	304			0.4	0.91	182
	0.45	0.41	82			0.45	1.28	256			0.45	0.61	122
	0.5	0.22	44			0.5	0.73	146			0.5	0.43	86
	0.55	0.08	16			0.55	0.55	110			0.55	0.18	36
	0.6	0.03	6			0.6	0.14	28			0.6	0.1	20
	0.63	0	0			0.63	0.08	16			0.63	0.05	10

Run 10	1 ml/min	25 C	3 Molar		Run 11	1 ml/min	90 C	3 Molar
11/23/2010	Voltage	Current	Cdensity		11/27/2010	Voltage	Current	Cdensity
	0.19	1.03	206			0.19	1.38	276
	0.24	0.85	170			0.24	1.23	246
	0.29	0.73	146			0.29	1.11	222
	0.35	0.51	102			0.35	0.93	186
	0.4	0.38	76			0.4	0.75	150
	0.45	0.22	44			0.45	0.53	106
	0.5	0.15	30			0.5	0.33	66
	0.55	0.03	6			0.55	0.13	26
	0.6	0.01	2			0.6	0	0
	0.63	0	0			0.63	0	0

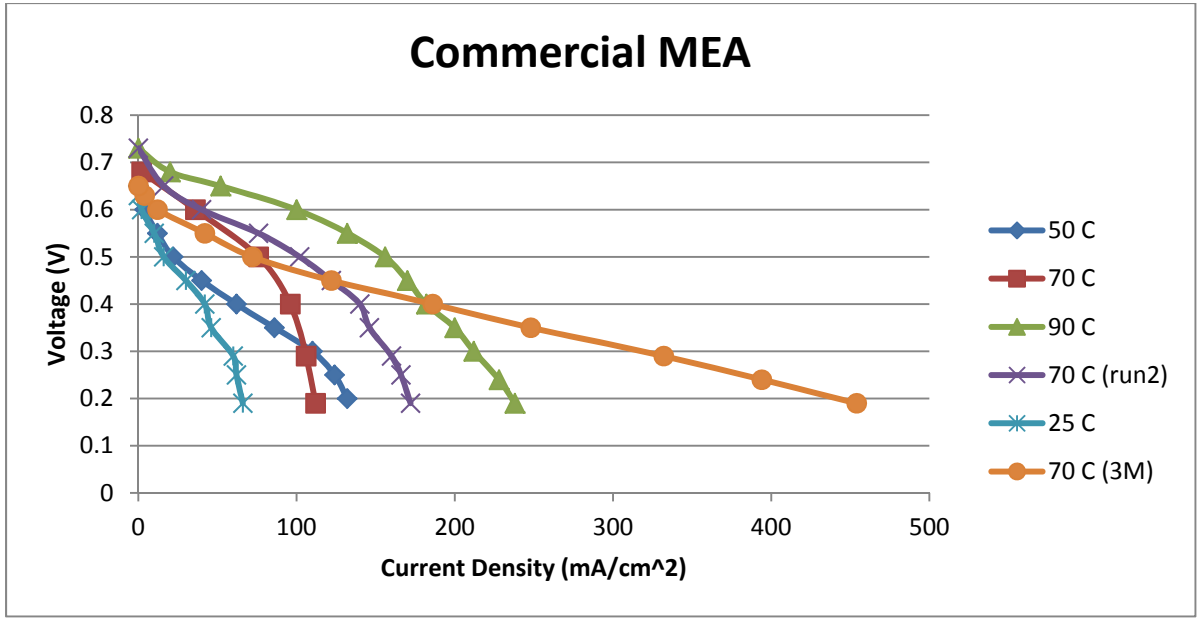
Commercial MEA
Voltage (V)
0.8
0.7
0.6
0.5
0.4
0.3
0.2
0.1
0
0
100
200
300
400
500
Current Density (mA/cm^2)
50 C
70 C
90 C
70 C (run2)
25 C
70 C (3M)

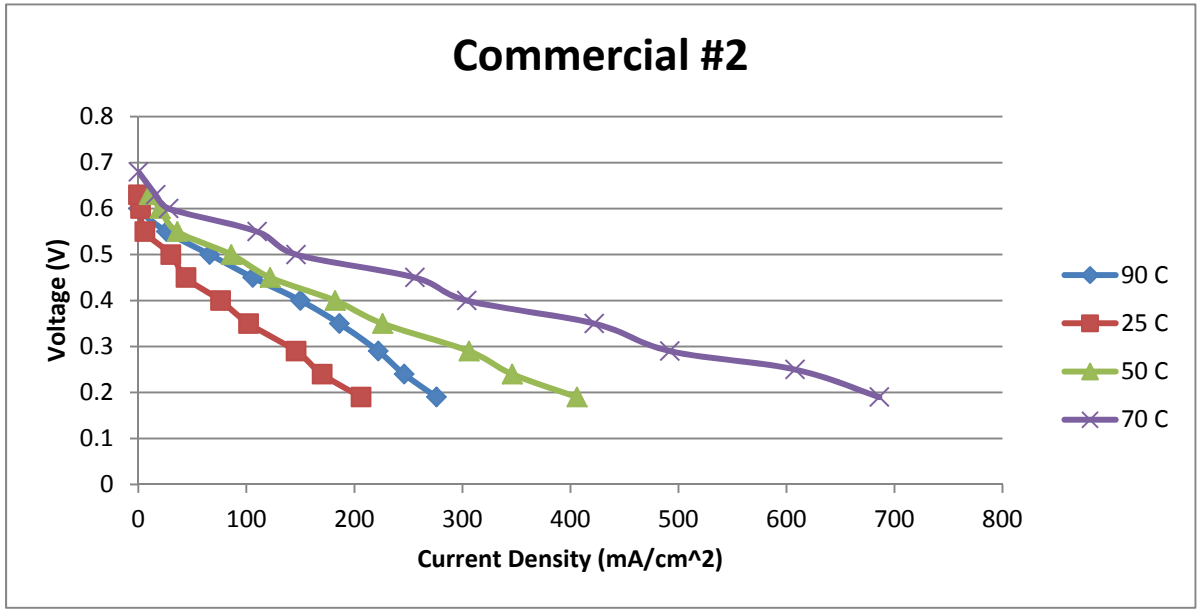
Commercial #2
Voltage (V)
0.8
0.7
0.6
0.5
0.4
0.3
0.2
0.1
0
0
100
200
300
400
500
600
700
800
Current Density (mA/cm^2)
90 C
25 C
50 C
70 C

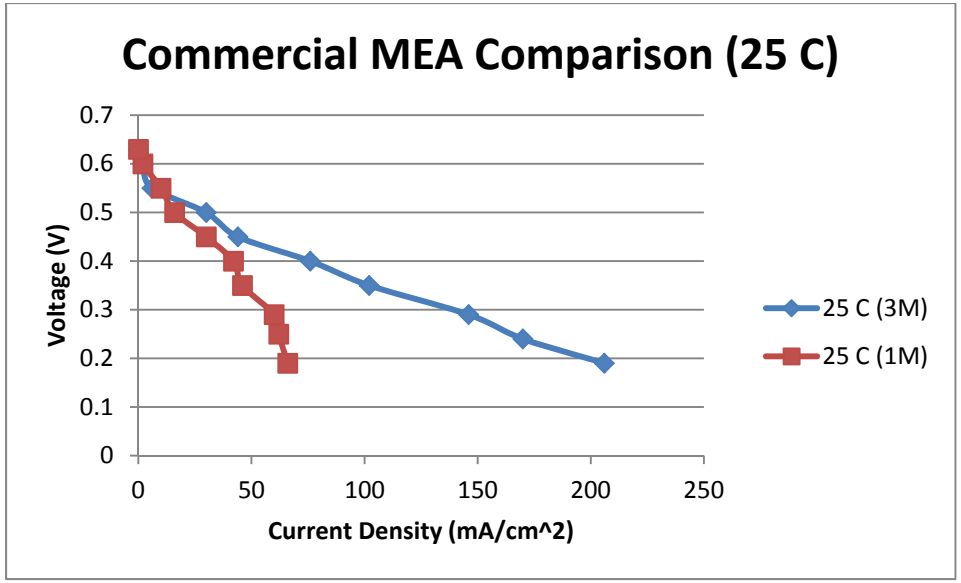
Commercial MEA Comparison (25 C)
Voltage (V)
0.7
0.6
0.5
0.4
0.3
0.2
0.1
0
0
50
100
150
200
250
Current Density (mA/cm^2)
25 C (3M)
25 C (1M)

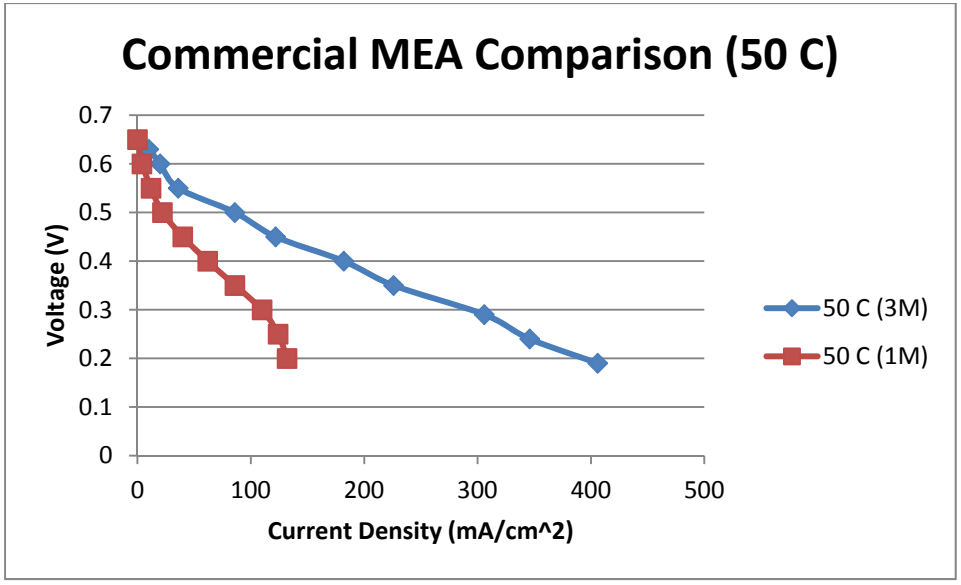
Commercial MEA Comparison (50 C)
Voltage (V)
0.7
0.6
0.5
0.4
0.3
0.2
0.1
0
0
100
200
300
400
500
Current Density (mA/cm^2)
50 C (3M)
50 C (1M)

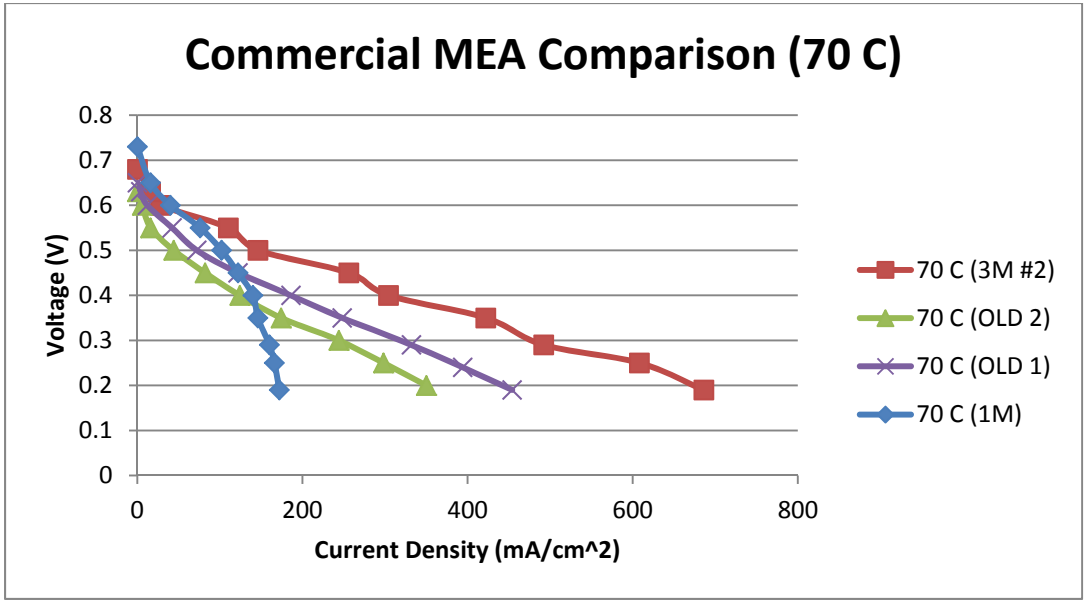
Commercial MEA Comparison (70 C)
Voltage (V)
0.8
0.7
0.6
0.5
0.4
0.3
0.2
0.1
0
0
200
400
600
800
Current Density (mA/cm^2)
70 C (3M #2)
70 C (OLD 2)
70 C (OLD 1)
70 C (1M)

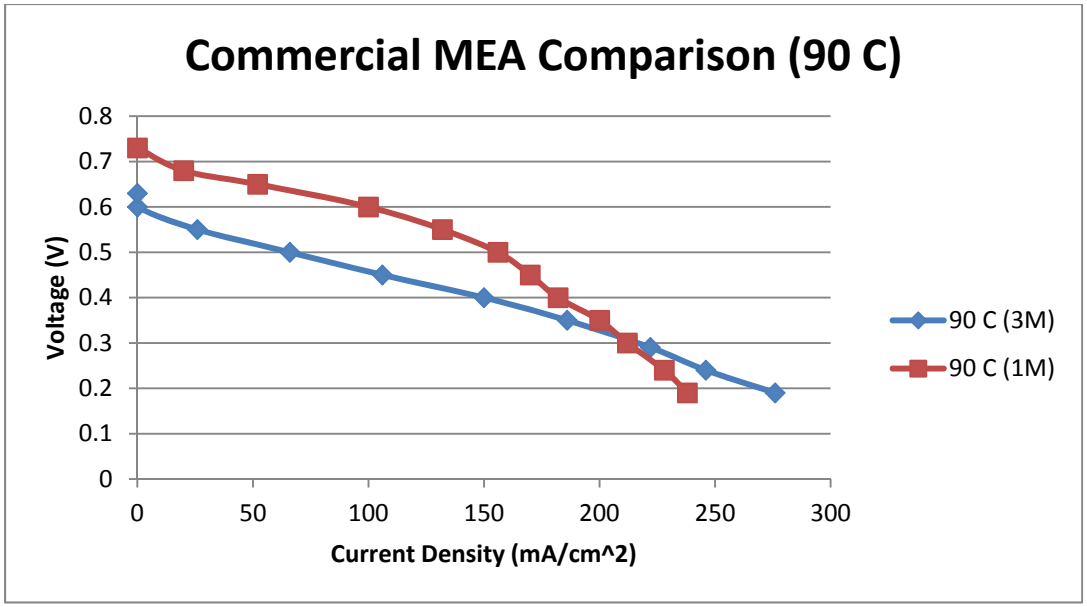
Commercial MEA Comparison (90 C)
Voltage (V)
0.8
0.7
0.6
0.5
0.4
0.3
0.2
0.1
0
0
50
100
150
200
250
300
Current Density (mA/cm^2)
90 C (3M)
90 C (1M)

Run 1	1 ml/min	70 C	3 Molar		Run 2	1 ml/min	50 C	3 Molar
12/8/2010	Voltage	Current	Cdensity		12/9/2010	Voltage	Current	Cdensity
	0.19	1.61	322			0.19	0.945	189
	0.24	1.405	281			0.24	0.845	169
	0.29	1.145	229			0.29	0.74	148
	0.35	0.805	161			0.35	0.585	117
	0.4	0.565	113			0.4	0.445	89
	0.45	0.345	69			0.45	0.295	59
	0.5	0.17	34			0.5	0.165	33
	0.55	0.065	13			0.55	0.055	11
	0.6	0	0			0.59	0	0

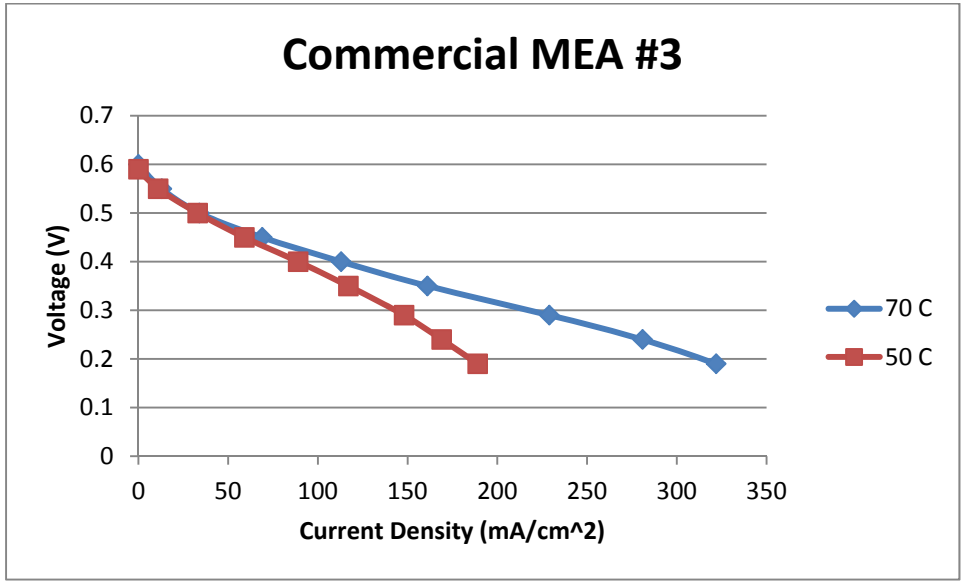

Appendix III: Consistency Data

2/5/2011	70 C	3M	2 ml/min		2/5/2011	70 C	3M	2 ml/min		2/6/2011	70 C	3M	2 ml/min
	0.2	2.2	440			0.2	2.27	454			0.19	2.17	434
	0.25	1.99	398			0.25	2.01	402			0.24	1.97	394
	0.3	1.74	348			0.3	1.81	362			0.29	1.72	344
	0.35	1.38	276			0.35	1.38	276			0.35	1.35	270
	0.4	1.09	218			0.4	1.05	210			0.4	1.02	204
	0.45	0.71	142			0.45	0.71	142			0.45	0.65	130
	0.5	0.43	86			0.5	0.45	90			0.5	0.34	68
	0.55	0.18	36			0.55	0.22	44			0.55	0.14	28
	0.6	0.06	12			0.6	0.11	22			0.6	0.03	6
	0.65	0.01	2			0.65	0.04	8			0.67	0	0
	0.68	0	0			0.68	0	0					

2/6/2011	70 C	3M	2 ml/min		2/7/2011	70 C	3M	2 ml/min
	0.19	2.21	442			0.19	2.22	444
	0.24	1.96	392			0.24	2.02	404
	0.29	1.71	342			0.29	1.76	352
	0.35	1.29	258			0.35	1.4	280
	0.4	0.96	192			0.4	1.04	208
	0.45	0.77	154			0.45	0.67	134
	0.5	0.33	66			0.5	0.35	70
	0.55	0.17	34			0.55	0.14	28
	0.6	0.09	18			0.6	0.03	6
	0.65	0.03	6			0.65	0	0
	0.67	0	0					

Appendix IV: Nafion MEA run with Hydrogen-Oxygen feed

4/12/2011	70C	H2-O2		4/13/2011	70C	H2-O2
Voltage	Current	Cdensity		Voltage	Current	Cdensity
0.19	1.19	238		0.19	1.18	236
0.24	1.13	226		0.24	1.11	222
0.29	1.1	220		0.29	1.03	206
0.35	0.95	190		0.35	0.95	190
0.4	0.85	170		0.4	0.85	170
0.45	0.78	156		0.45	0.76	152
0.5	0.65	130		0.5	0.66	132
0.55	0.56	112		0.55	0.58	116
0.58	0.4	80		0.58	0.51	102
0.68	0.18	36		0.68	0.28	56
0.78	0.05	10		0.78	0.08	16
0.9	0	0		0.9	0	0

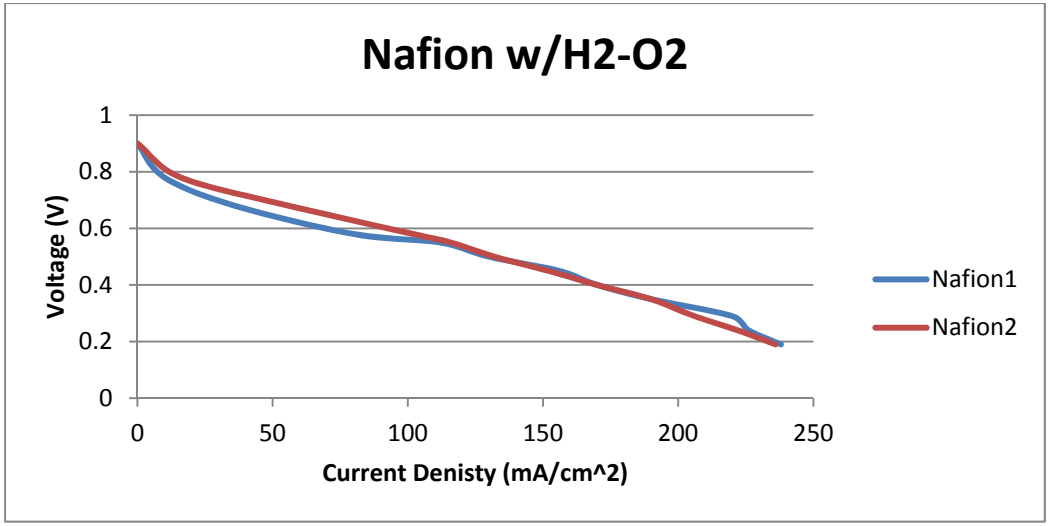
Nafion w/H2-O2
Voltage (V)
1
0.8
0.6
0.4
0.2
0
0
50
100
150
200
250
Current Denisty (mA/cm^2)
Nafion1
Nafion2

Appendix V: Gasket Thickness Calculation Table

BASF
The Chemical Company

Cell Gasket Thickness Calculation Table

unit: µm

MEA-thickness	Anode	Cathode	Total gasket thickness	Compression
700	250	300	550	21.4%
710	250	300	550	22.5%
720	250	300	550	23.6%
730	250	300	550	24.7%
740	250	300	550	25.7%
750	300	300	600	20.0%
760	300	300	600	21.1%
770	300	300	600	22.1%
780	300	320	620	20.5%
790	300	320	620	21.5%
800	320	320	640	20.0%
810	320	320	640	21.0%
820	320	320	640	22.0%
830	320	320	640	22.9%
840	320	350	670	20.2%
850	320	350	670	21.2%
860	320	350	670	22.1%
870	320	350	670	23.0%
880	350	350	700	20.5%
890	350	350	700	21.3%
900	350	370	720	20.0%

910	350	370	720	20.9%
920	350	370	720	21.7%
930	370	370	740	20.4%
940	370	370	740	21.3%
950	370	370	740	22.1%
960	370	370	740	22.9%
970	370	400	770	20.6%
980	370	400	770	21.4%
990	370	400	770	22.2%
1000	400	400	800	20.0%
1010	400	400	800	20.8%
1020	400	400	800	21.6%
1030	400	420	820	20.4%
1040	400	420	820	21.2%
1050	420	420	840	20.0%
1060	420	420	840	20.8%
1070	400	450	850	20.6%
1080	400	450	850	21.3%
1090	420	450	870	20.2%
1100	420	450	870	20.9%

Han Yu, 5/6/2010

Registered Place of Business:	Phone: +1 (732) 545-5100
BASF Fuel Cell, Inc.	Fax: +1 (732) 545-5170
39 Veronica Ave., Somerset, NJ 08873, USA	Internet: www.basf.com/fuelcell